MPPT Technique Based on Neural Network for Photovoltaic System

Elhor Abderrahmane

Master Degree In Renewable Energy and Energy Efficiency

Supervised by:

Prof. Orlando Soares
Prof. Kerboua Abdelfettah

Bragança 2021

MPPT Technique Based on Neural Network for Photovoltaic System

Dissertation presented to the Escola Superior de Tecnologia e Gestão do Instituto Politécnico de Bragança, made under the agreement of Double Diploma between the Polytechnic Institute of Bragança and Superior School of Applied Sciences of Tlemcen -Algeria- (ESSAT), to obtain the Master Degree in In Renewable Energy and Energy Efficiency

Acknowledgements

Dedication

To my dear Mother,

For her support and giving me invaluable advises through my entire life, I can't be where I'm without you.

To my dear Father,

For the continue giving me the encouragement, help, and sacrifices every day just to see me always successful. May this work reflect gratitude and happiness.

To my dear sister Fatima,

For your presence, support and your love.,

To all my dear brothers, Mostafa, Abdelmounaime and Adem and my dear sisters, Nacera and Ilham.

Hopefully, you are healthy, happy and enjoying your every moment in your life.

Abstract

The using of an efficient MPPT (Maximum Power Point Tracking) algorithm influences a lot in the global efficiency of the PV system. This thesis presents a detailed study based on simulation of different MPPT algorithms with their features using two systems (off-grid and on-grid). The off-grid system contains a PV array connected to a boost converter and a resistive load. On the off-grid system a simulation is presented using MATLAB/SIMULINK platform with several MPPT algorithms. The simulated MPPT algorithms are the conventionals Incremental Conductance (IncCond), Perturb and Observe (P&O), Open Circuit Voltage (OCV) and a new developed Neural Network (NN) under different environmental conditions of temperature and irradiance. As a result of the simulation, the NN algorithm has a quick response, i.e, it requires less time to reach the MPP and high efficiency and less oscillation comparing with the conventional methods. On the other hand, a single-phase two-stage photovoltaic grid-connected system is simulated which contains a PV array, a boost converter, a dc link capacitor, an inverter, an output L filter and the utility grid. In that system a control of dc link voltage, the injected current and the MPPT is made. Another MPPT algorithm based on NN (modified-NN) was also established. Showed later that is the most suitable for the system. The maximum of power is achieved when the irradiance is maximal and the temperature is minimal. Finally, a study of the influence of the variation in the climatic conditions on the output performance of the system is done.

Keywords:

MPPT, Neural Network, boost converter, PV system.

Resumo

O uso de um algoritmo de MPPT (Maximum Power Point Tracking-Rastreio do Ponto de Potência Máxima) eficiente influencia muito na eficiência global do sistema fotovoltaico. Esta tese apresenta um estudo detalhado com simulação de diferentes algoritmos MPPT com suas características utilizando dois sistemas (off-grid e on-grid). O sistema off-grid contém um painel fotovoltaico conectado a um conversor boost e uma carga resistiva. No sistema fora da rede, é apresentada uma simulação usando a plataforma MATLAB / SIMULINK com vários algoritmos MPPT. Os algoritmos MPPT simulados são os convencionais, Condutância Incremental (IncCond), Perturb e Observe (P&O), Tensão em Circuito Aberto (OCV) e uma nova Rede Neural (NN) desenvolvida sob diferentes condições ambientais de temperatura e irradiância. Como resultado da simulação, o algoritmo NN tem uma resposta rápida, ou seja, requer menos tempo para atingir o MPP, alta eficiência e menos oscilação em comparação com os métodos convencionais. Por outro lado, é simulado um sistema monofásico de dois estágios conectado à rede fotovoltaica que contém um painel fotovoltaico, um conversor boost, um barramento CC, um inversor, um filtro L de saída e a rede elétrica. Nesse sistema é feito um controle da tensão do barramento CC, da corrente injetada e do MPPT. Foi estabelecido também outro algoritmo MPPT baseado em NN (NN modificado) . Posteriormente foi mostrado que é o mais adequado para o sistema. O máximo de potência é alcançado quando a irradiância é máxima e a temperatura é mínima. Por fim, é feito um estudo da influência da variação das condições climáticas no desempenho de saída do sistema.

Palavras-chave:

MPPT, Rede Neural, conversor boost, sistema fotovoltaico.

Contents

List of Figures

List of Tables

List of abbreviations

C_{dc} dc link capacitor

C_i Input capacitor

C_o Output capacitor

f_{sw} Switching frequency

I_{cc} Short circuit current

i_{crr} Short-circuit current under STC conditions

i_d Current across the diode

I_{max} Maximum current

i_{ph} Photo-current

i_{pv} PV current

i_s Saturation current

K_i Temperature coefficient of the short-circuit current

L_f Output inductance filter

n_p Cells connected in parallel

N_s Number of cells connected in series

n_s Cells connected in series

P_{max} Maximum power

R_f output inductance filter resistance

r_p	Parallel resistor
r_s	Series resistor
V_{dc}	dc link voltage
v_d	Diode voltage
V_g	Grid voltage
V_{max}	Maximum voltage
V_{oc}	Open circuit voltage
v_{pv}	PV voltage
V_{rip}	voltage ripple
λ	Wavelength
ac	Alternative current
AI	Artificial Intelligence
A	Cell's area
C	Capacitor
dc	Direct current
E	Energy
f	Frequency
GD	Gradient Descent
G	Solar irradiance
h	Plank's constant
IncCond	Incremental Conductance
K	Boltzmann's constant
L	inductance

MPPT   Maximum Power Point Tracking

MSE   Mean Squared Error

NN   Neural Network

n   Ideality factor of the diode

OCV   Open Circuit Voltage

P&O   Perturb and Observe

PLL   Phase Locked Loop

PVG   Photovoltaic Generator

PV   Photovoltaic

q   Electron charge

SGD   Stochastic Gradient Descent

THD   Total Harmonic Distortion

T   Temperature

W   weight

w   Pulsation

Chapter 1

Introduction

1.1   Introduction

The energy consumption is growing in all regions of the world due to demographic development and industrialization. Currently, most of the production of electrical energy is based on non renewable resources like coal, natural gas and oil and those energy resources have harmful consequences on the environment.

So, the development of clean and renewable energy sources is needed, such as solar energy, wind energy, bioenergy...etc, because the renewable energies are inexhaustible, unlike non-renewable resources, which decrease over time. Renewable energies are still ecological and they contribute to the reduction of CO_2 emissions. In addition, they can be produced on a small-scale or locally.

Nowadays, the use of solar and wind energy presents a higher growth. But, if the advantages of these two types of energy sources are compared, it can be noticed that photovoltaic energy is preferred over wind, because it's daily production is almost regular, while the wind turbine is too intermittent due to wind activity, also the generator doesn't contain a moving parts and therefore practically the recurring operating and maintenance costs are relatively lower [1].

The solar energy has many applications and it's more flexible that is why it is more useful. Different equipment are connected with the photovoltaic generator to ensure the optimum transfer of energy. The power generated depends on temperature, irradiance and also the load. So, to make the photovoltaic generator works in its maximum power a MPPT (Maximum Power Point Tracking) algorithm must be implemented, with a lot of them are presented in literature.

1.2   Motivation

The nonlinear behave of the PV system makes the control of power more difficult. Also, the energy conversion efficiency depends on the type of PV cells used, the converters technologies (DC/DC or DC/AC), MPPT algorithm, and Healthy surrounding conditions for the system (dust, human-created shadow) [2].

The type of MPPT algorithm has a big influence in increasing the efficiency of the solar system. There's no perfect algorithm. the classic algorithms have a lot of drawbacks and the

major issue is the tracking while the meteorological conditions change rapidly [3].

So, the motivation is to develop an algorithm which can enhance the efficiency and gathers the advantages of a lot of techniques (the speed of tracking, the precision, stability, and keep tracking in suddenly environmental condition). The AI can be used to do this task by using an MPPT technique based on Neural Network (NN) with a multilayer feed forward perception type and the back-propagation algorithm for training.

1.3   The objective

This thesis is made a global view on the solar energy i.e, how the sun's irradiance is transformed to electricity (the photovoltaic effect) through the PV cell, also the different modelling, characteristics of the solar cell, the response of it in obscurity and under light conditions. The influence of the variation in the environmental conditions (irradiance, temperature) on the output power. The main objective of this thesis is to develop a Neural Network algorithm to track the maximum power starting by:

Firstly, using the platform of MATLAB/SIMULINK to connect the PV generator with the load through a boost converter. Control the switches of the DC/DC converter by a different MPPT algorithms (Incremental Conductance, Perturb and Observe, Open Circuit Voltage methods) and see the advantages and the drawbacks of each algorithm.

Secondly, the injection of the power produced in single phase two stage connected grid by ensuring the synchronisation between the injected current and the grid voltage. Ensuring an acceptable THD (Total Harmonic Distortion). This system controls the MPP, the dc link voltage and the injected current. Moreover, make a study about the influence of the variation in meteorological conditions on the output performance of the system.

Thirdly, develop a MPPT algorithm based on Neural Network by developing a multilayer feed forward perception and using the back propagation for training, in which an offline training must be ensured and validated before the using.

Finely, discussing the results and comparing the performance of the different MPPT algorithms covering the overshoot, time response, oscillation and stability.

1.4   The thesis's structure

This thesis is divided in five chapters organize as follows:

Initially, the first chapter begins by an introduction in which the necessity for going to the renewable energy is explained, especially solar energy. The motivation behind this thesis is presented. Finely, is explained the objective and the main target of this work.

The second chapter begins with an introduction on PV cells, then, is made a study on PV cells concerning the operating principle, their modeling and the different types of PV cells. Afterwards, is treated the influence of temperature and irradiance. Subsequently, the introduction of the PVG concept covering his design, features and the protection.

The third chapter presents an introduction about the MPPT algorithms and the different topologies used in the photovoltaic systems. The design of the boost converter with its parameters, equations and its circuit. Subsequently is shown the different features of the next MPPT algorithms P&O, IncCond and CV. After that, the Grid connected photovoltaic system with different topologies and components is established.

The fourth chapter starts with the introduction in which is described the need of intelligent system to control the MPP. So, is presented the Neural Network theory in general and its application in MPPT and the different steps for the implementation.

Finally, the fifth chapter is presented the different results including the off-grid and the on-grid systems. In both of them is discussed the different results of the four MPPT algorithms and also the different output and performances of two systems, finished by final conclusions and perspectives.

Chapter 2

State of art of the art

2.1   Introduction

The main element in the PV system is the solar cell which is the basic component of the PV panel. It's the responsible of converting the solar radiation into electricity. There's a various modeling examples of the photovoltaic cell presented in literature. Every cell is characterized by a lot of parameters depending on type of cell and the environmental conditions. The connection of several cells in series and parallel is used in PV module and different protection technologies are used in the PV module.

2.2   Photovoltaic cell

Since the PV cell is the main element of the PV system, it's necessary to highlight its functionality and the different used models which are described in this chapter.

2.2.1   The photovoltaic effect

The solar energy is the energy that comes from the sun, the photovoltaic cells convert that energy into electricity. This phenomenon is called the photovoltaic effect [4], the light enters a PV cell and imparts enough energy to some electrons (negatively charged atomic particles) to free them. A built-in-potential barrier in the cell acts on these electrons to produce a voltage (the so-called photovoltage) which can be used to drive a current through a circuit. The figure 2.1 presents the photovoltaic effect [5].
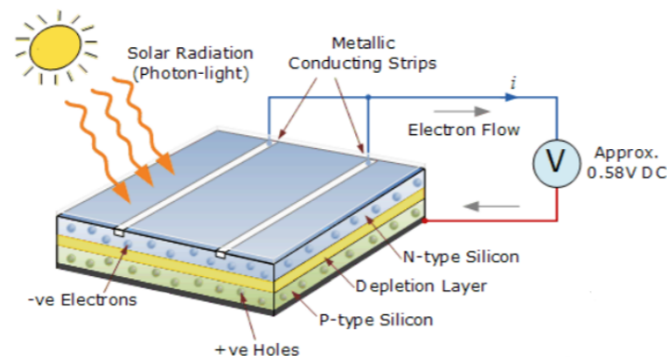
Figure 2.1: The photovoltaic effect.

A PV cell is a p-n semiconductor junction fabricated from semiconductor (usually silicon). Solar radiation is made up of particles called photons. A photon is characterized by its wavelength (λ) and energy (E):

$$E = h * \frac{c}{\lambda} \tag{2.1}$$

Where,

E: photon energy[J]

h: Plank's constant ($6,62607004 * 10^{-34}$ [J.s])

c: the speed of light (299 792 458 [m/s])

λ: wavelength of photon [m]

For generating a current, the energy of the photon must be greater than the gap of the material [6].

2.2.2   The functionality of the PV cell

When electrons get enough of energy they will move freely. But this movement can't generate a current because it's random. To make electrons follow one direction a driving force is needed and an easy and practical way to produce it is a p-n junction.

Similar to n type doping with Phosphorous P (five valence electrons) if the boron B is injected (three valence electrons) with silicon there will be one hole for each atom and this is called p type doping.

If these two kinds of doped materials are joined together, some electrons from the n side will migrate to the p region and fill the holes available there this way a depletion region is formed (no free electrons and holes). Due to electron migration the n side region becomes slightly positively charged and p side becomes negatively charged. An electric field will definitely be formed between the two charges this electric field produce the necessary driving force.

When the light strikes the n region of the PV cell and penetrates the depletion region the photon's energy is sufficient to generate electrons and holes pairs in the depletion region. The electric field in the depletion region drives electrons out of the depletion region. So, the

concentration of electrons in n region and holes in the p region become so high that the potential difference will develop between them as soon as any load is connected. Between the two regions electrons start flowing through the load. In this way the solar cell continually gives the direct current [7].

2.2.3   Modeling of a photovoltaic cell

To develop a precise equivalent circuit for a PV cell, it's necessary to understand the physical configuration of the elements as well as the electrical characteristics of each element. Many mathematical models have been proposed to represent the PV cell. The "one-diode model" , the "two-diode model" and the "polynomial model" [8]. The simplest circuit model is the "one-diode model" consisting of a current generator i_{ph} which is directly dependent on the solar irradiance (varies proportionally with the incident radiation [9]) and temperature, an antiparallel diode for cell polarization phenomenon, a series resistor r_S representing the voltage drop, a parallel resistor r_P characterizing the leakage current. The figure 2.2 shows the equivalent electrical circuit of the PV cell.
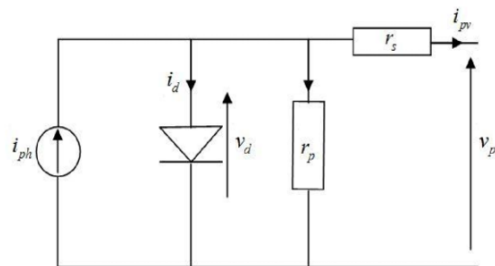
Figure 2.2: The equivalent electrical circuit of the PV cell.

Being,
i_{PV}: the PV cell current [A].
v_{PV}: the PV cell voltage [V].
i_{ph}: the photo-current [A].
r_S: the series resistor [Ω].
r_P: the parallel resistor [Ω].
i_d: the current across the diode [A].
v_d: the diode voltage [V].

Maximum power point

Based on the figure 2.7 it can be observed that the IV characteristic of the PV cell has a non-linear characteristic. A and B are the maximum power points for the real PV cell and ideal PV cell, respectively. The ideal PV cell present less of power losses than the real one.
The equation 2.2 shows the maximum power expression :

$$P_{max} = I_{max} * V_{max} \tag{2.2}$$

Maximum efficiency

It's the ratio between the maximum power and the incident light power as given in equation 2.3:

$$\eta = \frac{P_{max}}{P_{in}} = \frac{I_{max} * V_{max}}{A * G} \tag{2.3}$$

Where,

   A: is the cell area.

Fill factor (FF)

FF is the ratio of the maximum power that can be delivered to the load and the product of Isc and Voc as indicated in equation 2.4:

$$FF = \frac{P_{max}}{V_{oc} * I_{sc}} = \frac{I_{max} * V_{max}}{V_{oc} * I_{sc}} \tag{2.4}$$

The fill factor is a measure of the real IV characteristic, FF gives an idea about the aging process of PV cell, its value is higher than 0.7 for good cells [10] .

2.2.3.1 Case of an ideal PV cell

In this case, it is supposed that the series resistance r_S is small enough and the parallel resistance r_P is very high. Then, they can be neglected. The equivalent circuit of the ideal PV cell is shown in the figure 2.3.

The current expression in the diode under obscurity is given by:

$$i_{pv} = -i_d = -i_s[e^{\frac{q*V_{pv}}{(n*K*N_s*T)}} - 1] \tag{2.5}$$

(a) Under obscurity

(b) Under light

(a): Under obscurity.

(b): Under light.
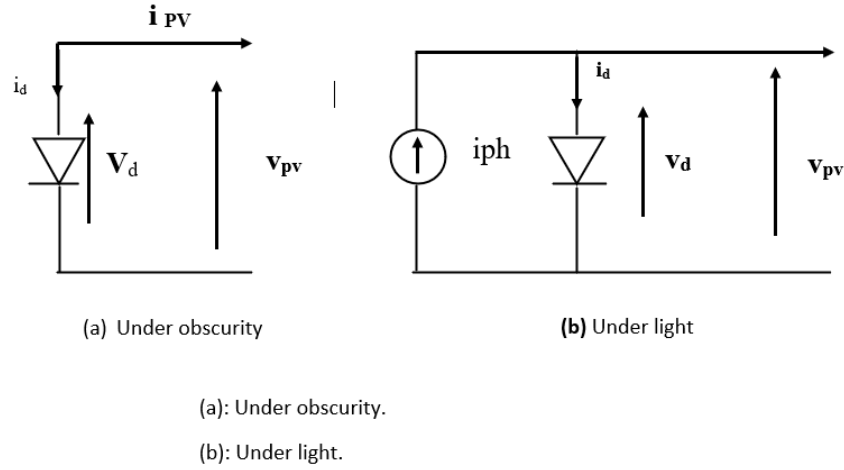
Figure 2.3: The equivalent electrical circuit of ideal PV cell.

Being,

i_s: saturation current [A]

q: electron charge $(1.6 * 10^{-19}$ [c])

n: the ideality factor of the diode

K: Boltzmann's constant $(1.38 * 10^{-23}[\text{J/K}])$

N_s: number of cells connected in series

T: operating temperature [K]

The current expression in the diode under light is given by:

$$i_{pv} = i_{ph} - i_d = i_{ph} - i_s\big[e^{\frac{q*v_{pv}}{(n*K*N_s*T)}} - 1\big] \tag{2.6}$$

The photo current expression is:

$$i_{ph} = \frac{G}{1000}[i_{scr} + K_i(T - 298)] \tag{2.7}$$

Being,

G: Solar irradiance in $[\text{w/m}^2]$

K_i: is the temperature coefficient of the short-circuit current (given by the constructor [A/K])

i_{scr}: is the short-circuit current under STC conditions (Gr=1000 w/m^2, Tr=25 C°)

To get the IV characteristic, a resistive load is used and each time the resistance value is

changed from very small resistance (I_{sc}, V=0) to very high resistance (I=0, V=V_{oc}). The figure 2.4 indicates the IV characteristic for an ideal pv cell.
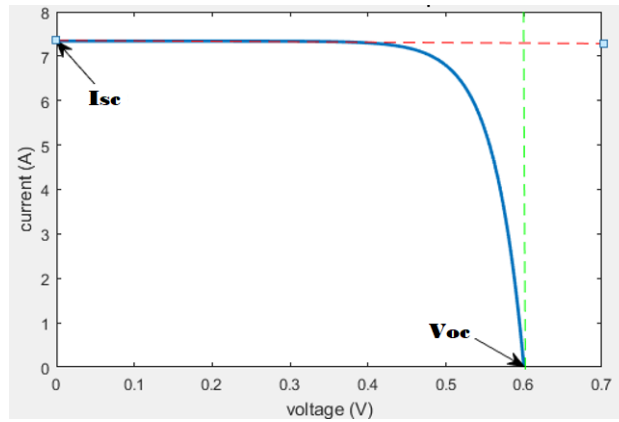
Figure 2.4: IV characteristic for an ideal PV cell.

2.2.3.2 Case of a real PV cell

In reality, the r_s resistance is in the order of a few milli-ohms and the r_p resistance is in the order of hundreds-ohms. So, they cannot be neglect and the equivalent circuit will be the one shown in figure 2.2. So, the expression of the current is given in equation 2.8:

$$i_{pv} = i_{ph} - i_d - i_p = i_{ph} - i_s [e^{\frac{q*(v_{ph}+ipv*r_S)}{(n*K*T)}} - 1] - \frac{vpv + ipv * r_S}{r_P} \qquad (2.8)$$

If is chosen r_s= 0.01 Ω and r_p= 439.1193 Ω, the IV characteristic for the real PV cell is as shown in the figure 2.5.
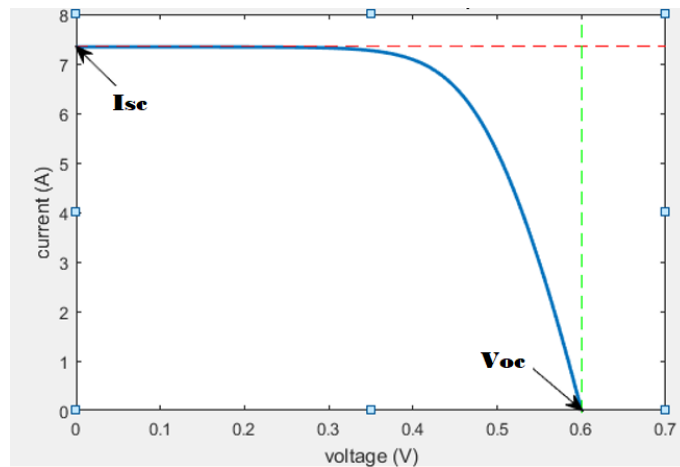
Figure 2.5: IV characteristic for a real pv cell.

The figure 2.6 and 2.7 indicate respectively the IV and PV characteristics for a real and ideal PV cells.
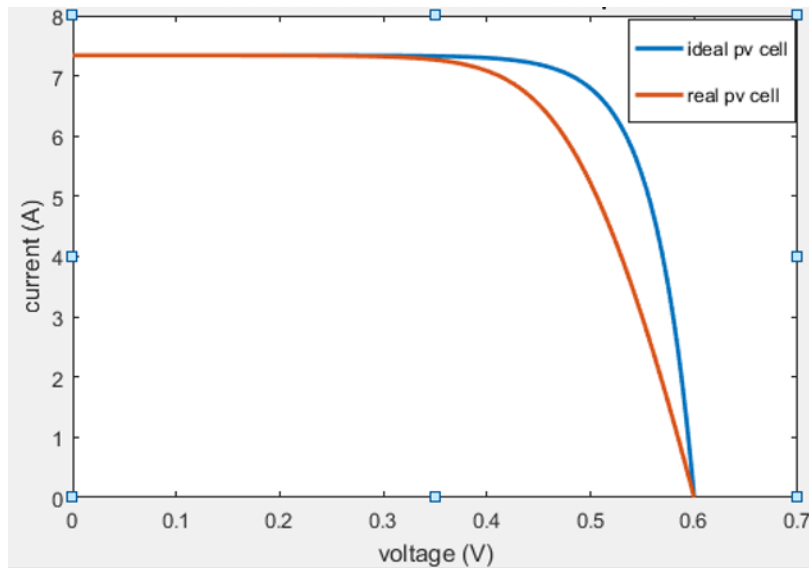
Figure 2.6: IV characteristic for an ideal and real PV cell.
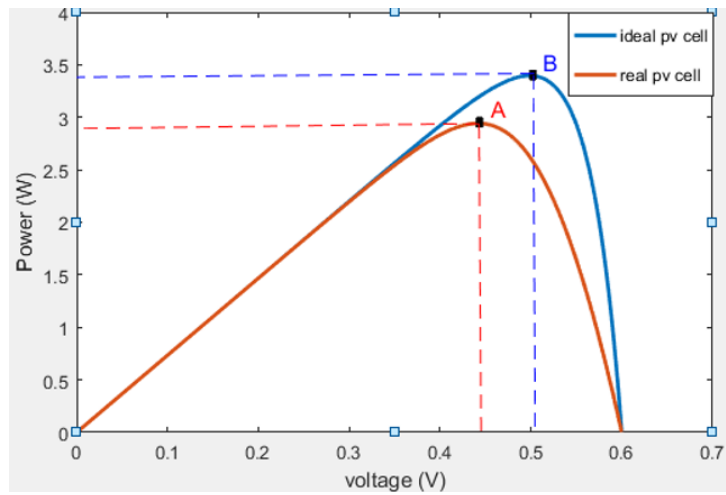
Figure 2.7: PV characteristic for an ideal and real PV cell.

It can be observed that the ideal PV cell provides high power than the real PV cell due to losses in the r_p and r_s resistances.

2.2.4 Influence of irradiance

The irradiance is an external parameter that depends on the exposure of the cell to the sun, it is the most influencing factor on the parameters of the cell. The photo-current is proportional to the irradiance (the equation 2.7) and opposed to the diode current.

The figure 2.8 shows IV and PV characteristics for a real PV cells on T=25°C:
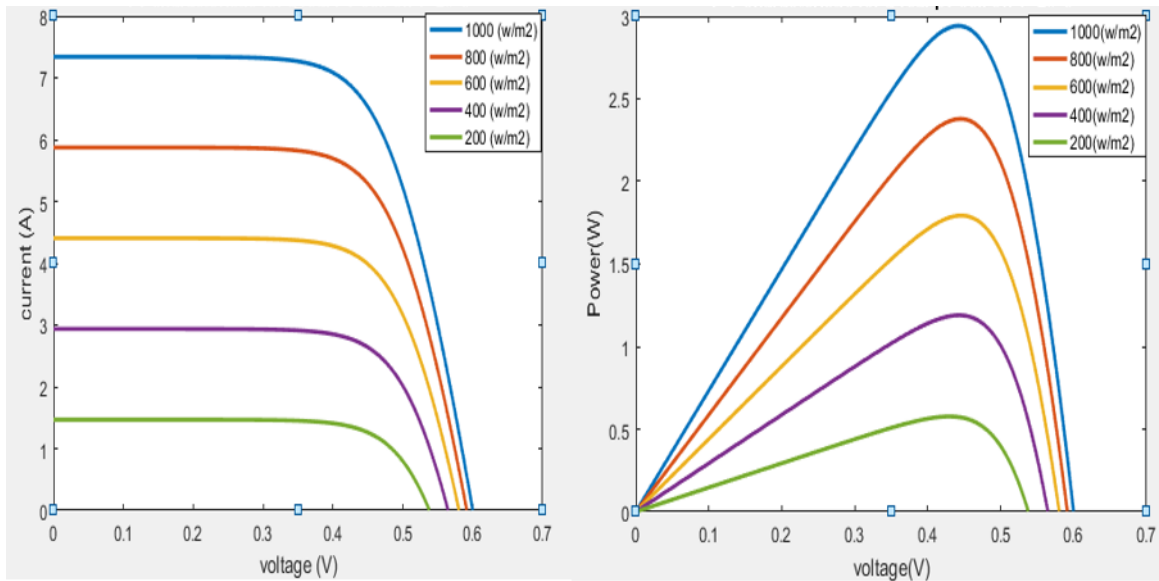
Figure 2.8: PV and IV characteristics for a real PV cell on T=25°C.

By varying the irradiance G, is noticed that the open circuit voltage V_{oc} has a small variation, contrary to the short-circuit current I_{sc} which varies a lot in function of the irradiance, which causes a huge variation in the power of the photovoltaic cell.

2.2.5 Influence of temperature

Temperature is the second most important parameter influencing the characteristics of the PV cell. The figure 2.9 shows IV and PV characteristics for a real PV cells under constant irradiance (G= 1000 $^{w}/_{m^2}$):
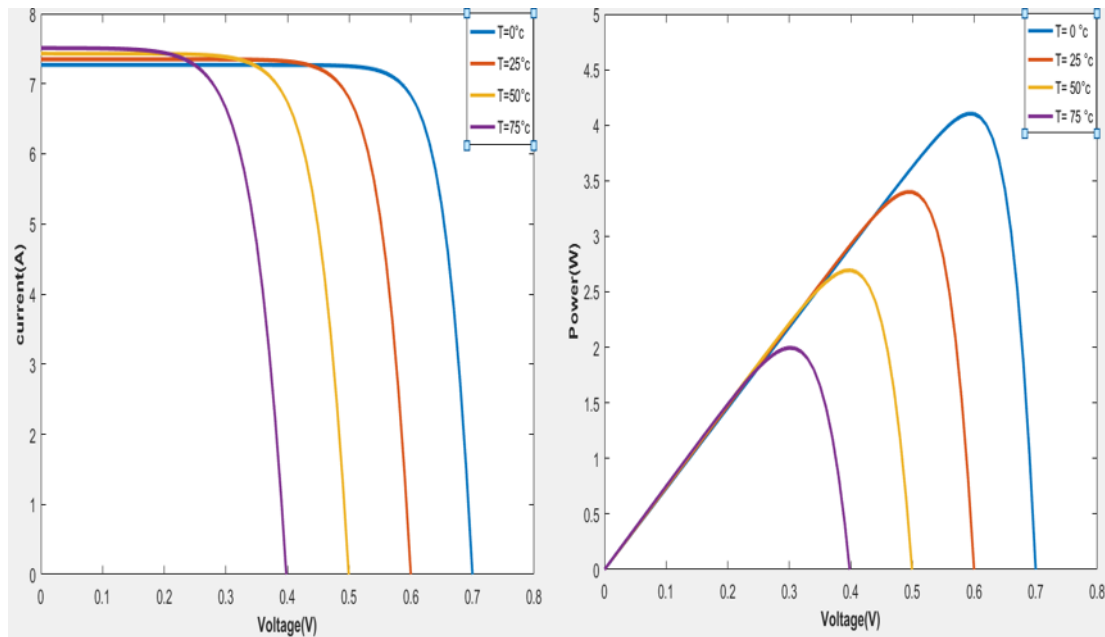
Figure 2.9: PV and IV characteristics for a real PV cell on G=1000 w/m^2.

Unlike the variation in irradiance, the variation in temperature mainly affects the open circuit voltage V_{oc}. When the temperature increases, the open circuit voltage decreases and vice versa.

The maximum power is achieved when we have a maximum of irradiance and a minimum of temperature.

2.3   Photovoltaic generator PVG

The photovoltaic cell is a low-power electrical generator, it's not sufficient for most domestic and industrial applications. In order to provide the necessary power for load a number of PV cells must be connected together in series and/or parallel to form a module.

2.3.1   Design and features of the PVG

The modules can be connected to each other in series and/or parallel to form photovoltaic generators (PV array) [1]. The figure 2.10 shows the constitution of a photovoltaic array [11].
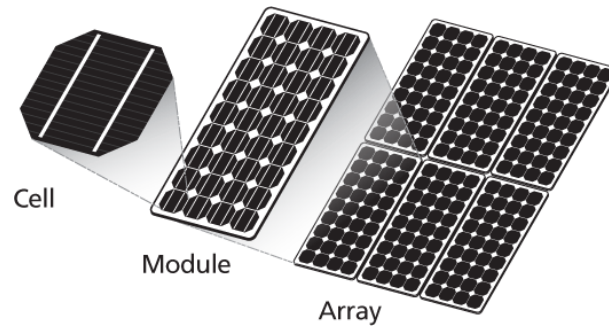
Figure 2.10: The constitution of a photovoltaic array.

An association of n_s cells in series increases the voltage, the cells will be crossed by the same current. The output voltage is the addition of every PV cell voltage as can be noticed from the next equation and figure 2.11.

$$\begin{cases} Voc_{ns} & = & n_s * Voc \\ Isc_{ns} & = & I_{sc} \end{cases} \tag{2.9}$$
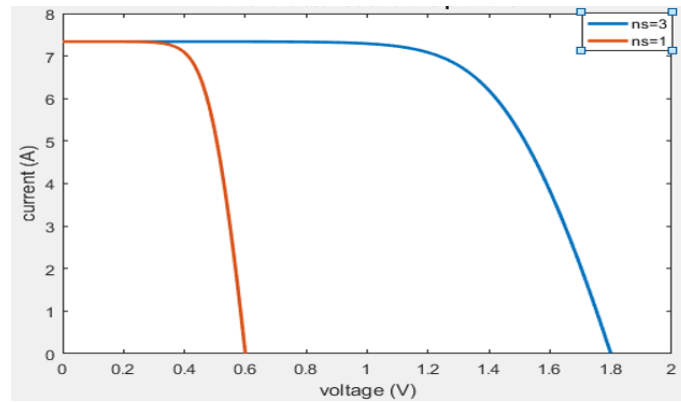
Figure 2.11: IV characteristic for n_s PV cells.

On the other side, a parallel association of n_p cells increases the current provided by the generator. A number of cells connected in parallel are under the same voltage. The output current is the addition of every PV cell current as presented in the equation 2.10 and the figure 2.12 .

$$\begin{cases} Voc_{np} & = & Voc \\ Isc_{np} & = & n_p * Isc \end{cases} \tag{2.10}$$
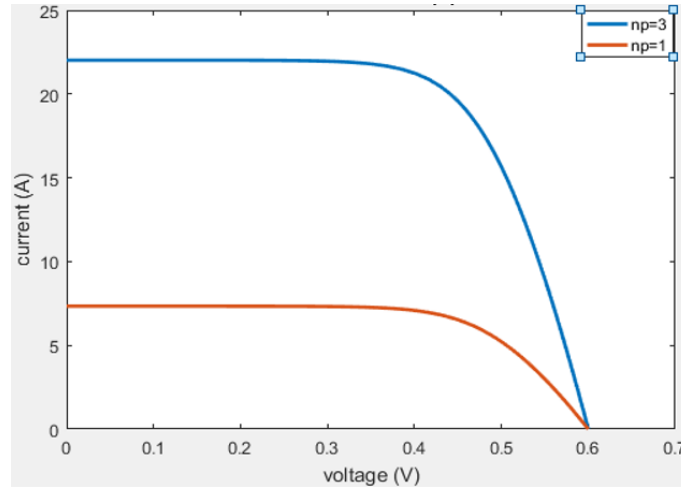
Figure 2.12: IV characteristic for n_p PV cells.

The operating voltage depends on the configuration of the power supply system, and the surface area of the module is variable depending on the constructor. The assembly of the modules in series and/or in parallel will make it possible to adjust different voltages and powers [11].

2.3.2 Protection of the PVG

To assure the continuity of supply under different conditions and to avoid damage of the PV cells there are two types of protection available:

1. Series

   The current flowing through the cells is the same and the voltages add up. Under non-uniform conditions of radiation for one cell of them, the cell may be submitted to the voltage of the other cells applied in reverse and it becomes like a receiver by dissipating a large amount of power and be destroyed if the break-down voltage of diode is exceeded. So, a diode must be connected in parallel (bypass-diode) to protect that cell. But, for Economic reasons adding a bypass diode to every cell isn't available. Therefor is placed

two bypass-diode for a normal thirty six cell module to avoid the **hot-spot** damage [12] in order to ensure the protection of cells with less bypass diodes.

2. Parallel

The cells are submitted to the same voltage and the currents add up. Under non-uniform conditions of radiation for one cell of them, the cell may be submitted to reverse current produced by the other cells and dissipate power and be destroyed. To prevent reverse current, a diode must be connected in series (blocking-diode) [12]. The figure 2.13 indicates the bypass diode and blocking diode.
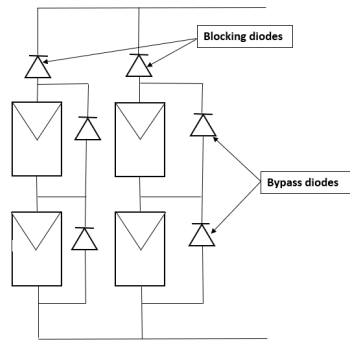
Figure 2.13: Bypass diode and blocking diode.

2.4 MPPT algorithms

Different MPPT methods have been published in the literature in order to achieve optimal performance. The most popular algorithm is perturb and observe (P&O) [13]. The incremental Conductance (IncCond) [14]. The open circuit voltage (OCV) also known as constant voltage method [15]. Also, another MPPT methods have been developed as fuzzy logic method [16] and genetic algorithm [17]. We find a MPPT algorithms based on Neural Network in [18], [19], [20] and [21]. Also, NN can be integrated with other algorithms as proposed in [22] and [23] . In [23] a partially shaded PV array controlled by a MPPT algorithm based on fuzzy logic and NN. The reference voltage given by the NN and fed the fuzzy logic system. This later, generates the required control signal for the power converter. The principal disadvantages of that system are the complexity and the high cost of implementation. In [24] a review of the most used MPPT algorithms covering: the direct methods (1) such as Incremental Conductance and Perturb and Observe and the indirect methods (2) such as Fractional Open-Circuit Voltage (FOCV) and

fractional short-circuit current (FSCC) and finally, soft computing methods (3) such as fuzzy logic control (FLC), a Kalman filter, Neural Network and partial swarm optimization (PSO). This later, also present detailed study of the advantages and drawbacks of each methods.

Chapter 3

Power electronics and MPPT algorithms

3.1   Introduction

As mentioned before, a PVG has non-linear IV characteristic. It admits a single point of optimal operation MPP (Maximum Power Point) in a constant irradiance and temperature. Each MPPT technique has its own features. A number of topologies are used for connecting PVG with load, each topology depends on the characteristics of the load. Also, the interconnection of photovoltaic systems to the grid needs an efficient converter to convert the low dc voltage to ac voltage [25].

3.2   Direct PVG-load connection

The direct connection of the PVG-load is the cheapest technique. The operating point of the PVG depends on the load impedance. It's the intersection between the IV characteristic of the PVG and the IV characteristic of the load. To avoid a negative current flow to the PVG, a blocking diode must be placed as shown in Figure 3.1.
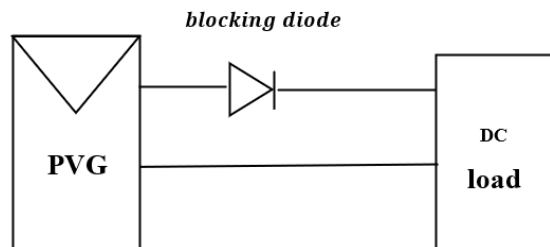
Figure 3.1: Direct PVG-load connection.

Let's take an example of a PV panel with different loads as shown in Figure 3.2.
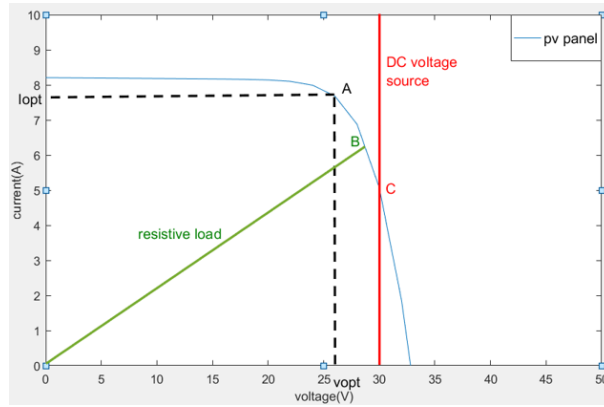
Figure 3.2: The Operating points of the PV panel according to the load in direct connection.

The figure 3.2 shows two types of loads connected directly to a PV panel:

- DC voltage source (battery).

- A resistive load.

For the operating points A, B and C, the output power of PV panel is respectively P_A, P_B and P_C. Both of P_B, P_C are lower than the maximum power P_A, the transmission of the maximum power is not available, the difference in power will be lost in PV panel as heat.

The maximum power produced by the PV modules varies according to variations in solar radiation, temperature and the connected load. Even in a constant temperature and irradiance there are different operating points.

Then, only a load whose characteristic passes through the point A (I_{opt}, V_{opt}) allows to extract the optimal power. The value of this load is then:

$$R_{opt} = \frac{V_{opt}}{I_{opt}} = f(G, T) \tag{3.1}$$

The optimal use consists in keeping the load at all times at its optimal R_{opt} value when conditions change. So, a power stage must be implemented to assure the optimal operating.

3.3   Power stages

To ensure the suitable PV array-load a power stage is needed. In the next section a study of DC/DC converters is performed.

3.3.1   DC/DC converters

There are many types of DC/DC converters can be connected with the PV generator according to the load voltage (Buck, Boost and Buck Boost).

The connection via a power stage shown in the figure 3.3:
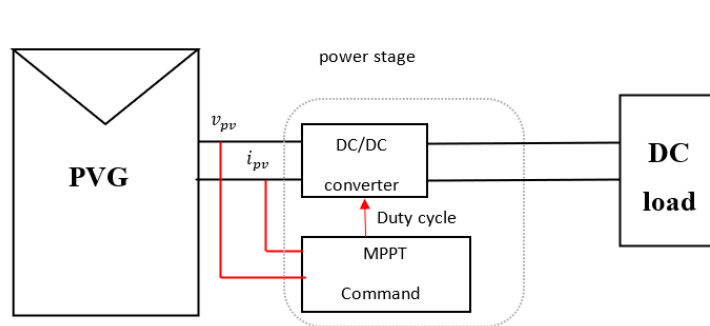
Figure 3.3: PVG-load connection via power stage.

The boost converter will be used as a power stage.

The boost converter

The boost converter is a power converter with a dc output voltage higher than its dc input voltage. It contains two semiconductors (diode, switch) and at least one energy storage element. The output capacity is added to reduce output voltage ripple. Also, the boost converter is called a step-up converter. The figure 3.4 indicates the circuit of the boost converter.
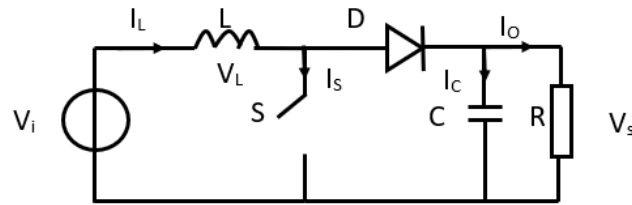
Figure 3.4: The circuit of the boost converter.

The figure 3.5 shows the switch's state:
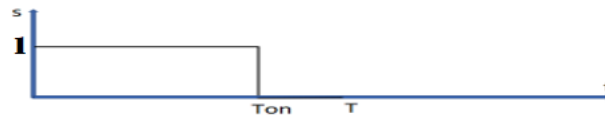
Figure 3.5: The state of the switch.

We define the duty cycle as: $D = \frac{T_{on}}{T}$

$[0, T_{on}]$: The switch (S) is closed, the inductance current increasing progressively, the inductance stores up energy. The figure 3.6 presents the boost converter in the on time.
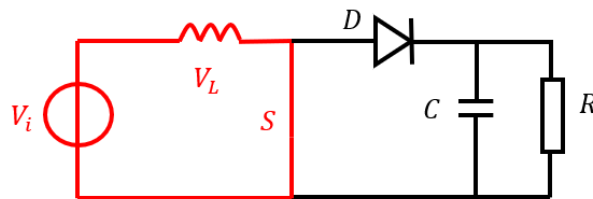
Figure 3.6: The boost Converter during on time.

The voltage across the inductor is:

$$V_i = V_L \tag{3.2}$$

The mathematical equation characterizing the inductance current is given by:

$$\frac{dI_L}{dt} = \frac{V_i}{L} \tag{3.3}$$

$[T_{on}, T]$: The switch (S) is open, the inductance generates a voltage which is added to the source voltage, which is applied to the load (R) through the diode (D). The figure 3.7 presents the boost Converter during off time.
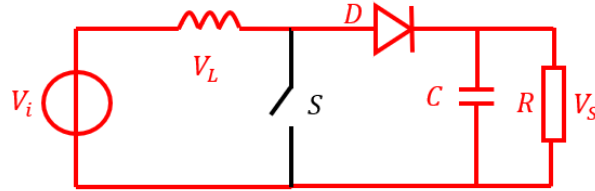
Figure 3.7: The boost Converter during off time.

The voltage across the inductance is:

$$V_L = V_i - V_S \tag{3.4}$$

The mathematical equation characterizing the inductance current is given by:

$$\frac{dI_L}{dt} = \frac{V_i - V_S}{L} \tag{3.5}$$

The average value of the voltage V_L is zero:

$$< V_L >= \int_0^T V_L dt = 0 \tag{3.6}$$

So,

$$< V_L >= (V_i)(D * T - 0) + (Vi \smile Vs)(T - D * T) = 0 \tag{3.7}$$

Then,

$$V_S = \frac{V_i}{1 - D} \tag{3.8}$$

With:

$$I_o = I_i(1 - D) \tag{3.9}$$

The design of the boost converter inductance depends essentially in the current ripple which is inversely proportional to the inductance value as shown in the next equation [26] .

$$L = \frac{V_i * D}{\Delta I * f_{sw}} \qquad (3.10)$$

On the other side, some types of loads require an alternative voltage source, but the PV panel generates direct current, so, the direct connection is not possible in this case.

3.3.2   DC/AC converter

To supply an AC load from a PVG, an inverter must be used as an adapter stage. Indeed, an inverter is a power electronics device that allows an AC voltage to be delivered from a DC source. The structure of an inverter usually consists of electronic switches such as IGBTs, power transistors or thyristors. In order to obtain an alternating signal of a specific frequency, the source is modulated by means of switches generally controlled by pulse width modulation (PWM) [1].

3.4   MPPT algorithms

The use of MPPT algorithms is indispensable to have a PV system with high efficiency. The next suctions highlight different MPPT algorithms.

3.4.1   Introduction

The determination of the maximum power is more delicate as it depends of meteorological parameters (temperature and irradiance). As a result, it becomes more difficult to operate the system at maximum power. So, a command for the tracking of the MPP is required, this command is known as the MPPT algorithm. It is generally based on adjusting the duty cycle of the static converter until it reaches the MPP. In the next sections a detailed steady of some MPPT algorithms with their features is presented.

3.4.2   Perturb and observe algorithm (P&O)

The P&O method is the most popular MPPT algorithm due to its simplicity [27]. It's one of the **Hill climbing** algorithms. The objective of this algorithm is to operate the system at

it's maximum power by incrementing or decrementing the voltage at the operating point and observing the effect of this perturbation on the power. The table 3.1 shows the response of the control system for each case:

Case n°	ΔV	ΔP	$\frac{\Delta P}{\Delta V}$	Direction of tracking	response of the control
1	+	+	+	good	Incrementing: $V_{ref} = V_{ref} + V$
2	-	-	+	bad	Incrementing: $V_{ref} = V_{ref} + V$
3	+	-	-	bad	Decrementing: $V_{ref} = V_{ref} - V$
4	-	+	-	good	Decrementing: $V_{ref} = V_{ref} - V$

Table 3.1: The response of the control system for each case of P&O algorithm.

Different cases are shown in the figure 3.8.
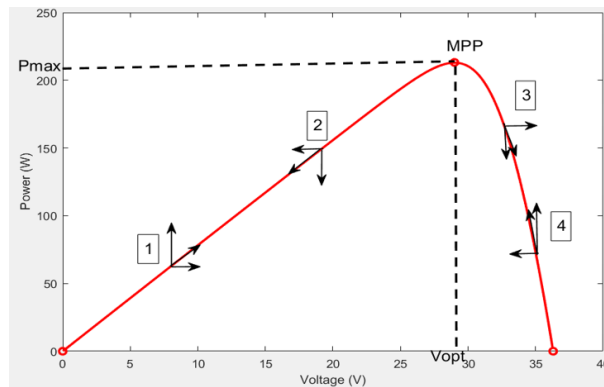
Figure 3.8: The different possible cases for the functioning of P&O algorithm.

The P&O algorithm has the advantages of precision and speed of response; however, this method may suffer from fast changes in environmental conditions [28], the fluctuation in steady state around the MPP. The figure 3.9 shows the flowchart of the P&O algorithm.
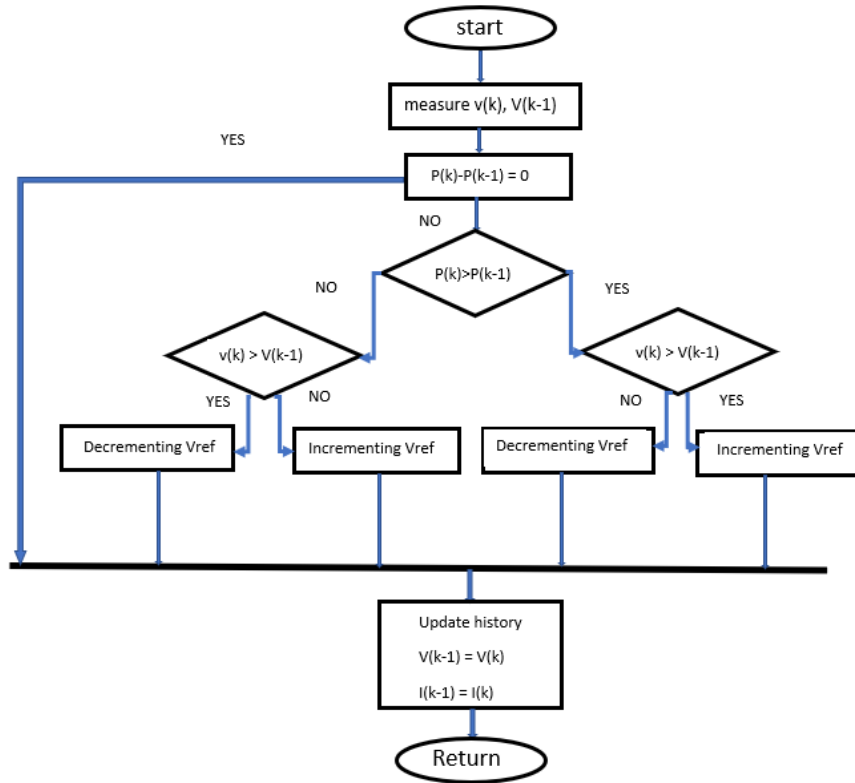
Figure 3.9: The flowchart of P&O method.

3.4.3   Incremental Conductance (IncCond).

Incremental Conductance is also one of the techniques of **Hill climbing**. Where the MPPT command tries to raise the operating point of the PV generator along the PV characteristic until it reaches MPP. It based on the principle that the slope of the PV array power curve is zero at the MPP($\frac{dP}{dv} = 0$) . It searches for MPP based on equality of conductance (Y=$\frac{I}{V}$) and conductance increment (Y=$\frac{\Delta I}{\Delta V}$).

$$\frac{dP}{dV} = \frac{d(VI)}{dV} = I\frac{dV}{dV} + V\frac{dI}{dV} = I + V\frac{dI}{dV} \approx V\frac{\Delta I}{\Delta V} + I \qquad (3.11)$$

Where,

$$\begin{cases} \frac{\Delta I}{\Delta V} = -\frac{I}{V} & if \qquad \quad P \quad in \quad the \quad MPP \\ \frac{\Delta I}{\Delta V} < -\frac{I}{V} & if \quad P \quad in \quad the \quad right \quad of \quad MPP \\ \frac{\Delta I}{\Delta V} > -\frac{I}{V} & if \quad P \quad in \quad the \quad left \quad of \quad MPP \end{cases} \qquad (3.12)$$

By comparing the conductance and the conductance increment, three operating point positions can be detected which are presented in figure 3.10.
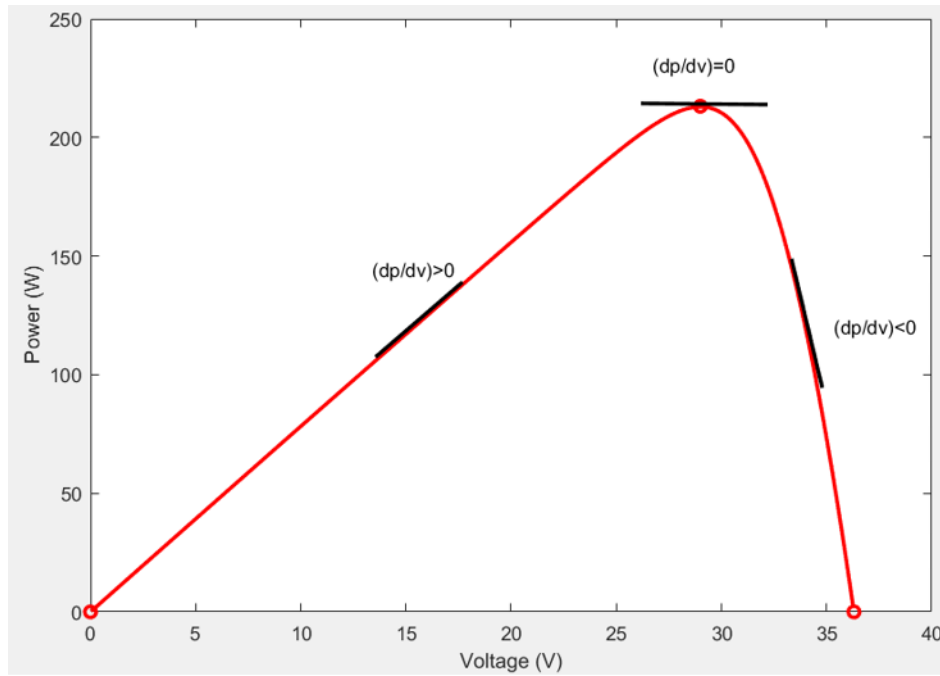
Figure 3.10: The operating points of the IncCond method.

The figure 3.11 presents the flowchart of IncCond method.
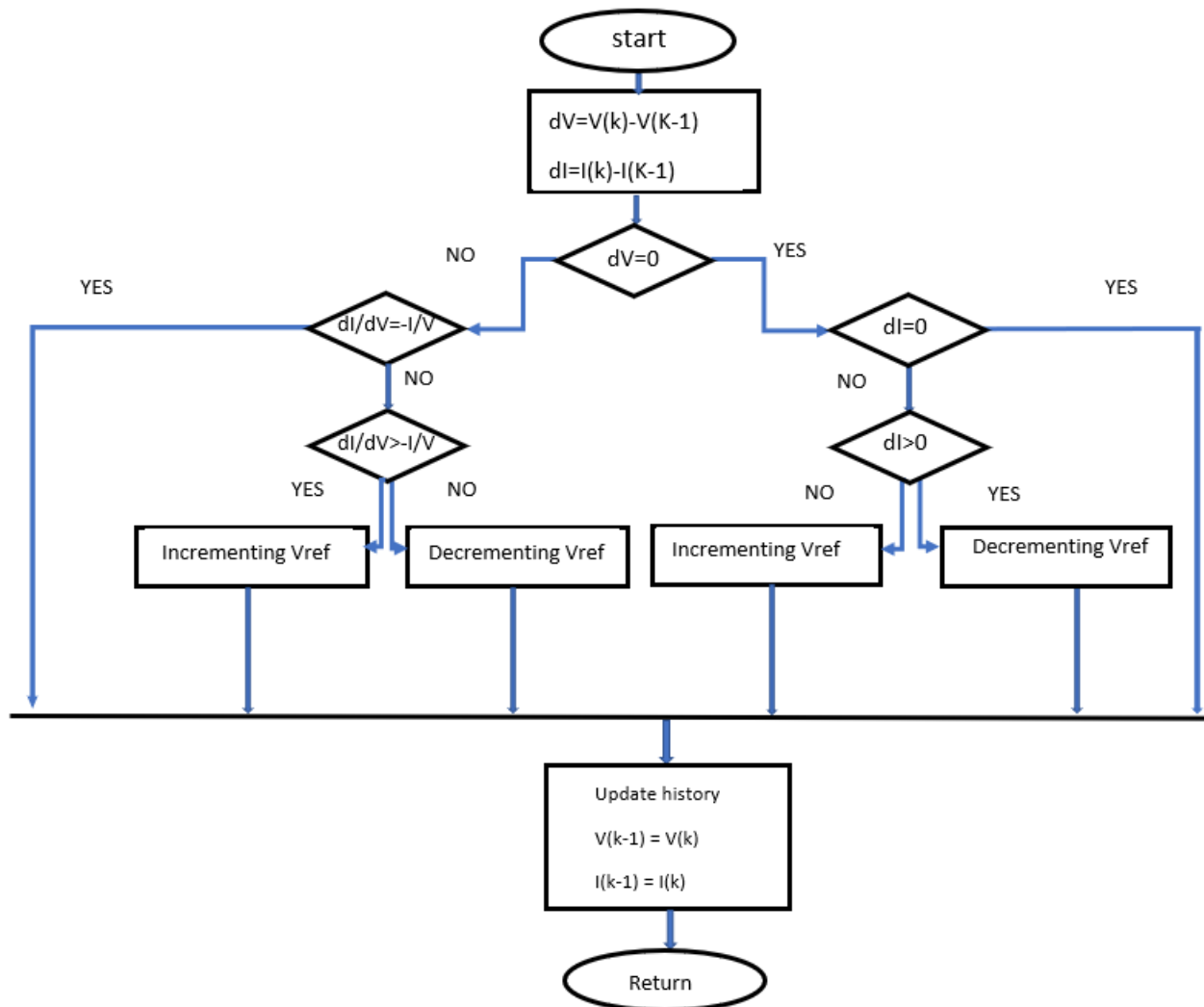
Figure 3.11: The flowchart of incremental conductance method.

The advantages of this algorithm are the precision and speed of the MPP search when atmospheric conditions change rapidly. The implementation of this algorithm presents difficulties due to the complexity of the control circuit and the real-time calculation of the derivative requires a fast calculation processor [29]. In other terms, the execution of the IncCond algorithm requires more time compared to P&O. In practice, even the IncCond method has oscillations around the MPP [30].

3.4.4   The open circuit voltage method (OCV)

The open circuit voltage method (OCV) is the simplest algorithm to achieve MPP based on the open circuit voltage. Such that the voltage at MPP (V_{MPP}) is around 70%–80% of the PV open-circuit voltage (V_{OC}) [28] ($K = \frac{V_{MPP}}{V_{OC}} = 70\% - 80\%$). It has a very fast response time. This method is characterized by its rapidity and poor tracking under different conditions.

The figure 3.12 shows the flowchart of the OCV algorithm.
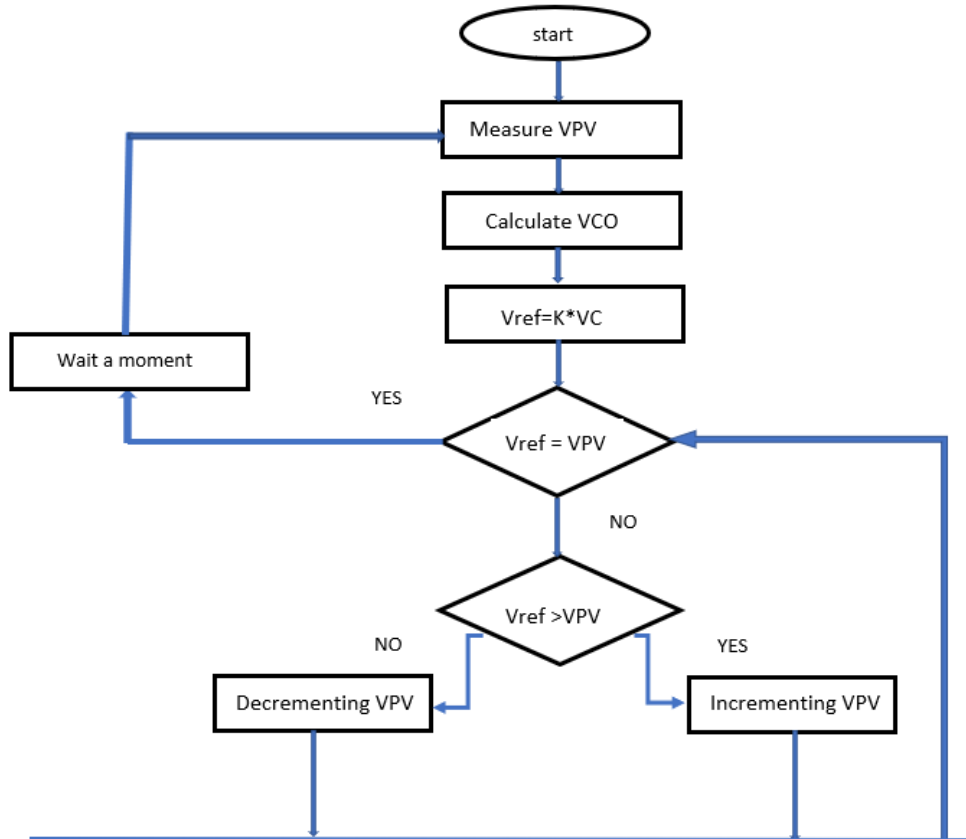
Figure 3.12: The flowchart of OCV method.

To get the V_{OC} of the panel and avoid the cutting in power a reference cell can be proposed. The reference cell is similar to the cells of the PV panel. Every time the V_{OC} of reference cell is achieved, the number of cells in series is multiplied by the open circuit voltage of the reference cell and multiply the result by a coefficient ($K = \frac{V_{MPP}}{V_{OC}}$).

3.5   Grid connected photovoltaic system

The grid photovoltaic connection is made in three phases or in single phase connection. This thesis focus on the study of the single-phase connection. The injection of the solar energy in the grid is growing up due to the reduction in cost when eliminating batteries [31]. For the grid connected photovoltaic system the inverter current produced should has the same phase and frequency of the utility grid [32].

3.6   Single Stage Inverter

The PV system is directly connected to the inverter which connected to the grid. The single stage has two tasks: the extraction of the maximum power point and the injection of sinusoidal current to the grid [33]. That configuration is simple and reduce the cost however presents a lot of drawbacks like the non-flexibility of the structure, low efficiency compared to two stage inverter [34]. The figure 3.13 shows the structure of single stage system.
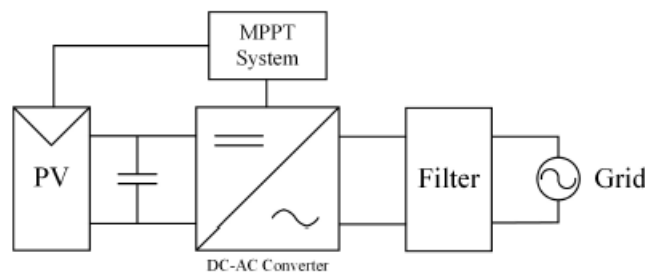
Figure 3.13: The structure of single stage system.

3.7   Two Stage Inverter

To improve the design flexibility and the poor extraction of energy. As a single stage, the DC/DC converter is implemented between the PV array and the inverter. The DC/DC converter can be used to reach the MPP and adjust ripple DC voltage.The second stage is the DC/AC converter which injects the sinusoidal current to the grid. The figure 3.14 presents the structure of two stage system.
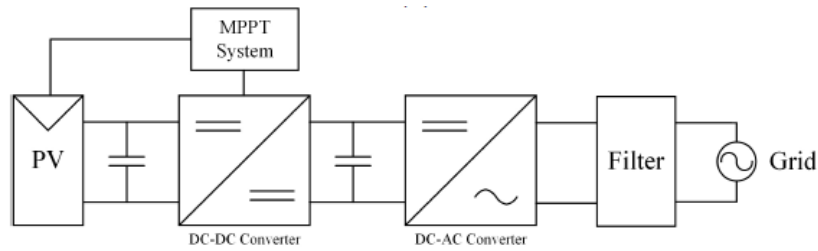
Figure 3.14: The structure of two stage system.

3.8   The phase locked loop (PLL)

To connect the inverter to the utility grid it's necessary to ensure that both of the PV inverter and the grid are synchronized, i.e, they have the same frequency, phase and the same amplitude [35]. Is a feedback control system, that automatically adjusts the phase of a locally generated signal to match the phase of an input signal. Consequently, providing a unit power factor operation [36]. The figure 3.15 shows the general structure of a single-phase PLL [36].
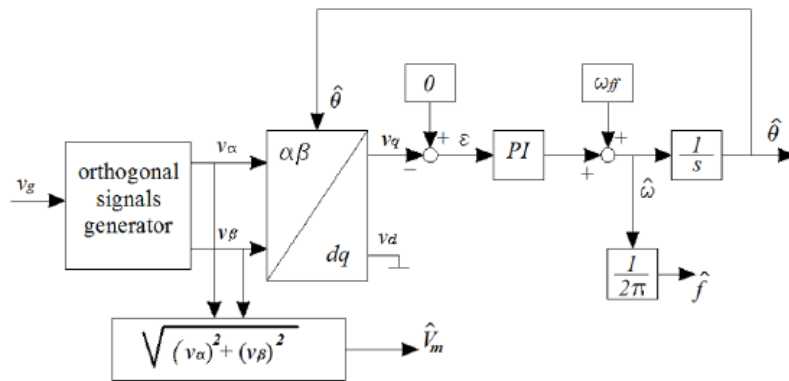
Figure 3.15: The general structure of a single-phase PLL.

3.9   Low-pass Output Filter for on-grid PV Inverter

In the grid connected photovoltaic inverter the presence of the harmonics around the switching frequency provides a problems in the inverter current. For this reason, the PV system requires an output low-pass filter to connect with the utility grid [37]. In the literature,

L-filter, LC-filter and LCL-filter designs have been proposed. The most popular low pass filter is L filter due to the simplicity of design comparing with the second order filter (LC filter) and third order filter (LCL filter) configuration [38].

For a unity power factor and the unipolar Pulse Width Modulation (PWM), the value of the inductance L can be calculated as [37]:

$$L = \frac{v_{dc}}{4 I_{rated} \Delta_{ripple} f_{sw}} (1 - m_a) m_a \tag{3.13}$$

Where I_{rated} is the rated utility current, Δ_{ripple} is the maximum ripple magnitude percentage (5% - 25%), v_{dc} is the dc-link voltage, L is the total filter inductance; f_{sw} is the switching frequency (Hz) and m_a is the modulation index.

In the sinusoidal pulse width modulation technique the modulation index is given by [38]:

$$m_a = \frac{v_{ref}}{v_c} \tag{3.14}$$

Where v_{ref} is the reference signal amplitude and v_c is the carrier wave signal amplitude.

3.10   Voltage source inverter (VSI) control

The control of the VSI based on the phase shift between the inverter output voltage and the grid voltage. The control of active and reactive power injected are achieved by the current control techniques. Several algorithms of the current control are present in the literatures: Hysteresis, predictive, and sinusoidal pulse width modulation (SPWM). The control of VSI based on SPWM presented in [39]. This control method has the advantage of applying very simple digital circuits, the control of active and reactive powers injected [40]. Hysteresis current control strategy presents robust current regulation, achieve unity power factor, low THD and optimize the PV energy extraction suitable for grid connected PV systems [41].

3.11   The control algorithm for single-phase two-stage photovoltaic grid-connected system

Getting high power quality and high operation efficiency is an essential aim in the PV system connected to the grid. A double grid-frequency voltage ripple is an issue in single-phase

photovoltaic grid-connected systems founded on the dc link because of the unbalance of the instantaneous dc input and ac output powers [42]. As a result, increasing of the total harmonic distortion (THD) in the injected current. For a good power quality, the THD in the injected current must be less than 5% [43]. The next control algorithm controls the MPP, the dc link voltage and the injected current. Consequently, the system works in MPP, reducing THD and improving the quality of the output power.

3.11.1 The system configuration

A single phase two stage photovoltaic grid connected system presented in figure 3.16 [42]. The first stage presents a boost converter. The control of the boost converter is ensured by an MPPT algorithm. A dual loop controller controls the second stage (the H-bridge inverter). The outer loop controls the dc-link voltage to follow the reference value (V_{ref}) and it has like output the maximum value of the reference current (i_{ref}). A phase-locked loop (PLL) generates the grid voltage phase. A unit-amplitude sinusoidal signal is synchronised with the grid voltage and multiplied by the maximum magnitude of the reference current to get a unity power factor. The inner loop (current control loop) makes the inverter current follow the current reference.
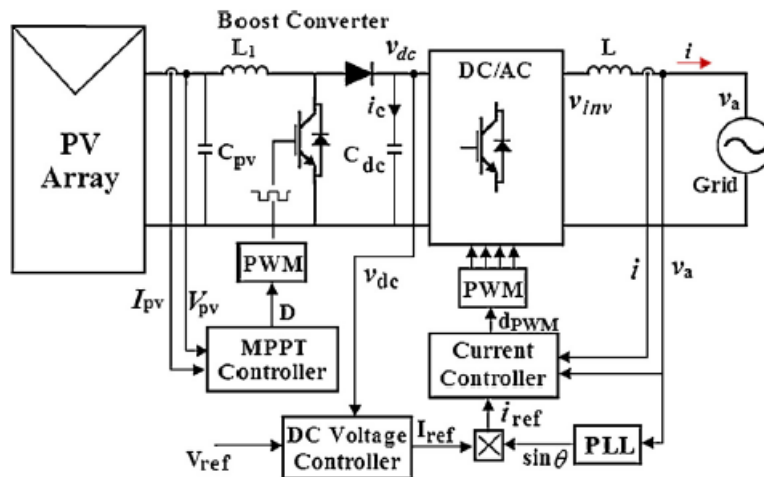
Figure 3.16: A single phase two stage photovoltaic grid connected system.

3.11.2 The double grid-frequency voltage ripple source

Considering that a unity power factor is achieved:

$$v_a = V_m sin(wt) \tag{3.15}$$

$$i = I_m sin(wt) \tag{3.16}$$

So then,

$$P_o = V_m I_m sin^2(wt) \tag{3.17}$$

$$P_o = \frac{V_m I_m}{2}(1 - cos(2wt)) = \frac{V_m I_m}{2} - \frac{V_m I_m}{2}cos(2wt) \tag{3.18}$$

The first term of equation 3.18 is the average ac power injected to grid. On the contrary, The second term describes the oscillations of the alternating current which is the source of the double ripple of the grid frequency.

The DC input power of inverter is given by:

$$P_{inv} = P_{pv} - i_c v_{dc} \tag{3.19}$$

$$P_{inv} = P_{pv} - C_{dc} V_{dc} \frac{d\Delta v_{dc}}{dt} \tag{3.20}$$

we suppose the inverter has a unity efficiency following this:

$$P_{inv} = P_o \tag{3.21}$$

So,

$$P_{pv} = \frac{V_m I_m}{2} \tag{3.22}$$

$$\frac{d\Delta v_{dc}}{dt} = \frac{V_m I_m}{2C_{dc} V_{dc}}cos(2wt) \tag{3.23}$$

So then,

$$\Delta v_{dc} = \frac{V_m I_m}{4w C_{dc} V_{dc}}sin(2wt) = V_{rip}sin(2wt) \tag{3.24}$$

We can see from the equation 3.24 that the voltage ripple depends inversely proportional with the dc link capacitor size and the dc link voltage.

The sizing of the dc link voltage ripple is given in several papers [44] and [45] as:

$$\Delta v_{dc} = \frac{Po}{w C_{dc} V_{dc}} \tag{3.25}$$

As mentioned in [42], the increasing of the voltage ripple causes a Raising of the total harmonic distortion as a result getting poor power quality. Instead, the increasing of the capacitor size reducing the voltage ripple as shown in equation 3.25 and raising the cost of the grid connected inverter.

Chapter 4

Neural Networks

4.1   Introduction

In the way of improving the performances of the MPPT. Some algorithms are proposed such as what have been described in the previous chapter. One of the modern MPPT techniques is the Neural Network (NN) algorithm which is inspired from the biological nervous systems. Which is branch of artificial intelligence (AI). In this chapter, will be presented Neural Networks theory, the using of NN for the MPPT and the different steps for the implementation in the system.

4.2   Neural Network theory

Before using the network several steps must be followed to validate and test the network as shown in the next sections.

4.2.1   Neural Network definition

It's a lot of simple elements working in parallel. The connections between those elements create a network. The goal of that network is to predict an output based on the training of the network used inputs and targets. Every single connection between two neurons has a weight which is used to adjust the network, i.e, change the weights until the outputs achieve the targets [46]. Currently NN is used in various fields for example identification, classification, speech, vision and control systems [47].

4.2.2   Neuron model

The artificial neuron is an elementary processor. It connects with the input through a weight. Every neuron has one output (a) and associated with a transfer function (f) [48]. There are some neurons also associated with bias (b) which is a simple scalar or like a weight (W) with input equal to one [47]. The next figure shows the structure of an artificial neuron:
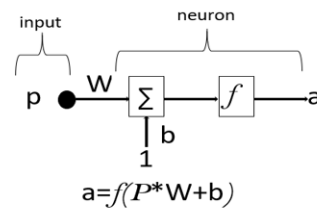
Figure 4.1: The structure of the neuron with one input.

The structure of neuron with multiple inputs is shown in the next figure:
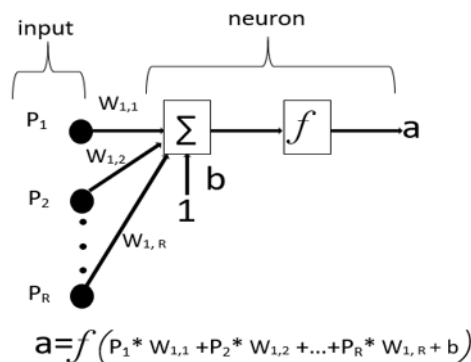
Figure 4.2: The structure of the neuron with R inputs.

4.2.3   Transfer functions

There are a lot of transfer functions the most used are:

The **hard-limit** transfer function, which returns a 0 or a 1, is shown Figure 4.3.

The **linear** function is a neural transfer function. Transfer functions calculate a layer's output from its net input. The equation 4.1 indicates the linear transfer function.

$$f(x) = x \tag{4.1}$$

The equation 4.2 describes the **log-sigmoid** transfer function.

$$f(x) = \frac{1}{1 + e^{-x}} \tag{4.2}$$
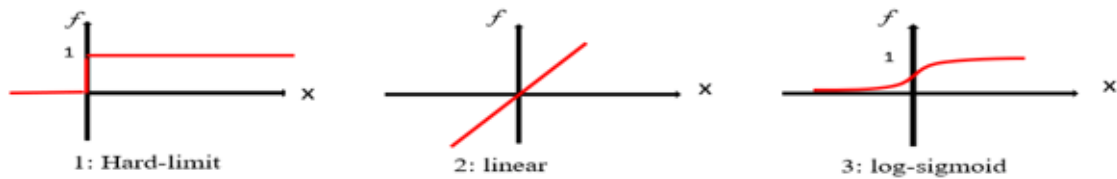
Figure 4.3: The most transfer functions used.

4.2.4   Network architectures

Several neurons create a layer. The connection between these layers forms a network. The layer that is directly attached to the inputs is called **the input layer** . The layer that connected with the output is known as **the output layer**. n invisible layers are referred as **the hidden layers**. The first topology of networks developed is **Feedforward** which has a definition that every neuron of layer can connect only with the neuron of the next layer. On the other hand, the **Feedforward with shortcut connections** is a network which allows the neuron to have a connection with neurons in different layers [49]. The figures 4.4 and 4.5 present the Feedforward and Feedforward network with shortcut connections networks respectively.
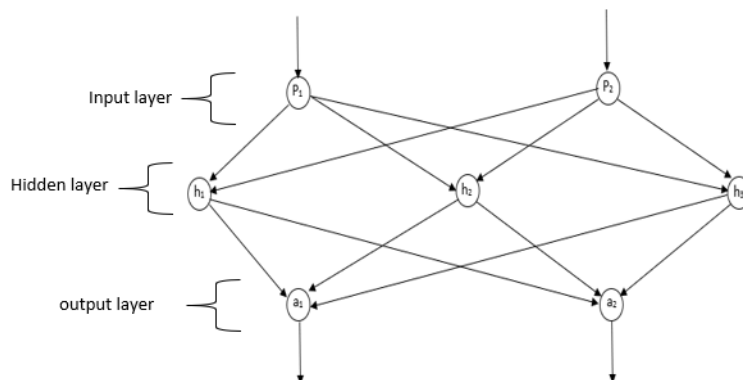
Figure 4.4: Feedforward network.
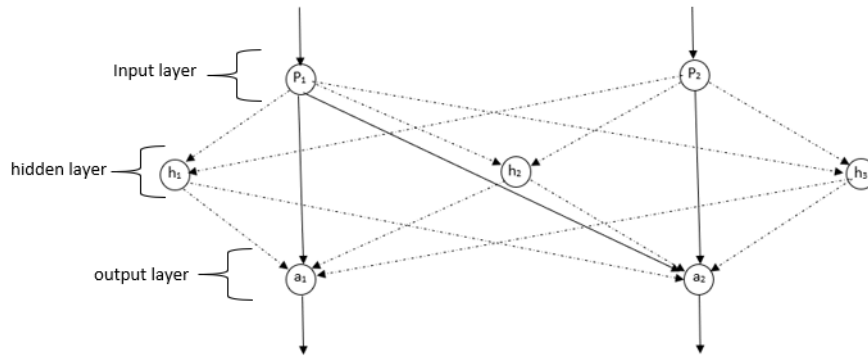
Figure 4.5: Feedforward network with shortcut connections.

4.2.5   Neural Network Design Steps

The good Neural Network results obtained by the right training. The standard steps for designing neural networks is given bellow [50] .

- Data collection.

- Selection of network structure

- Training the network.

- Testing the network.

4.2.6   The Mean Squared Error MSE

The validation of the network justified by the convergence of the output to the target i.e, a small MSE [50].

$$MSE = \frac{1}{N} \sum_{k=1}^{N} (t_i - a_i)^2 \tag{4.3}$$

Where,

N: the number of outputs.

t: target.

The reduction of MSE obtained by adjusting the weights. So, the needs of back-propagation algorithm.

4.2.7   The back-propagation algorithm

The Back-propagation algorithm is an iterative method where the network evolves from an initial unlearned state to a fully learned state [51]. The Gradient Descent (GD) is the first one developed by Rumelhart (1986) [52]. However, it's impractical for example, in the case of a lot of samples it was observed that training with the Stochastic Gradient Descent (SGD) is more generalized than with GD [53].

The learning phase of the multi layer network consists of adapting the weights of the connections based on the prediction errors found [54]. It can be distinguished two steps, the first one, The calculation of the derivatives error function MSE (W) with respect to the weights. In the second step, the derivatives are then utilized to establish the adjustments to be made to the weights [52]. After the two steps can be seen the effect of each weight over the the prediction error and which weight has a big influence in reducing the error.

4.3   The MPPT based on Neural Network

The Neural Network is used to make the system works in MPP. The proposed method is based on sensing the most important factors which influencing in the power (irradiance, temperature) and controlling the system by varying the duty cycle. So:

The inputs : irradiance, temperature.

The outputs : duty cycle.

The figure 4.6 shows the architecture of the proposed method.
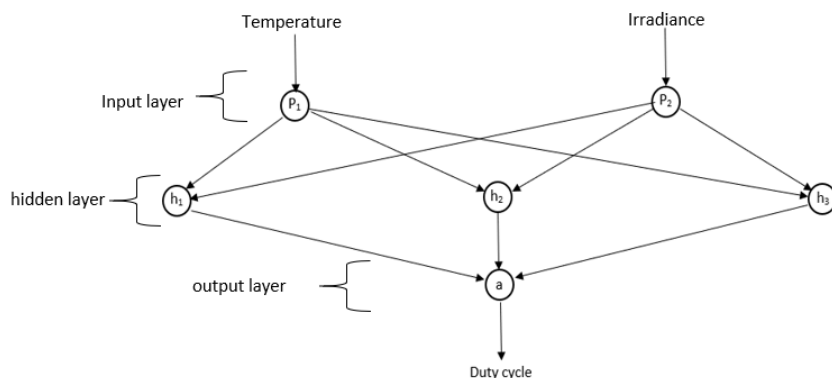
Figure 4.6: The proposed NN algorithm.

As mentioned previously in 4.2.5 the network must be well trained before used (at offline training). The all steps of getting the network are explained below:

4.3.1   Data collection

The first step in designing an ANN is to collect data (inputs, outputs). Getting more data enhance the performance of NN. In our case lots of solar irradiances and temperatures and their corresponding duty cycle ratios are taken. The samples are obtained by varying the irradiance and temperature inputs of the PV array and getting values of duty ratios. With supervised learning, was used tagged data, i.e, a collection of data that already has been known, to determine a learning algorithm [55].

4.3.2   Selection of network structure

The structure and the configuration of the network influence on the results. The choice of NN structure means setting all the parameters of Network, i.e, the type of network, the number of layers, the number of neurons in each layer and the activation function. In addition, Log-Sigmoid Transfer Function is usually used in back-propagation network because it's differentiable [48]. Until now, there are no guidelines method for deciding the number of layers and neurons needed, it is about varying them until reach the best results [56].

4.3.3   Training the network

After setting the NN design, the collecting data are provided for training. The training algorithms using the training function to adjust and update the weights. There are many of them presented in literature for example: Gradient descent back-propagation, One-step secant back-propagation, BFGS Quasi-Newton back-propagation and Levenberg-Marquardt back-propagation [57]. The corresponding algorithm the one that has a small MSE, i.e, the predicting duty cycle converge to the real duty cycle of MPP.

4.3.4   Testing the network

Testing the network is the last step before using the network, in this step the weights are constants (no changing in the network structure), just measure the network performance. If there are non accurate results or poor performance the network must be retrained, it can adjusted the performance of NN by increasing the number of samples, changing the training algorithm, increase the number of neurons [58]. In the case of outliers, which are data points where the fit is significantly worse than the majority of data, is needed to check the validity of those data, if they are a good data is needed to extrapolate the network by getting more data similar to them. In the other case they will be deleted.

Chapter 5

Results and discussion

In order to make a comparison between the different MPPT algorithms, two systems are proposed:

(1) Off-grid system which contains: a PV array ensures the photovoltaic conversion. A Boost converter is connected with the PV array to elevate the voltage; the control of the Boost converter is ensured through an MPPT algorithm to make the system operates in the maximum power point, and a resistive load is connected with the boost converter.

(2) On-grid system which contains a PV array, a DC/DC boost converter, an inverter and utility grid. The MATLAB/SIMULINK platform is used for simulation. The simulated methods are P&O, IncCond, OCV, the proposed NN and the modified NN. All simulation results and discussion are presented in this chapter covering overshoot, time response, oscillation and stability.

5.1   Off-grid system

In the way of getting the different features of the MPPT algorithms, an off-grid is simulated in a different environmental conditions. The figure 5.1 presents the architecture of the system explained before.
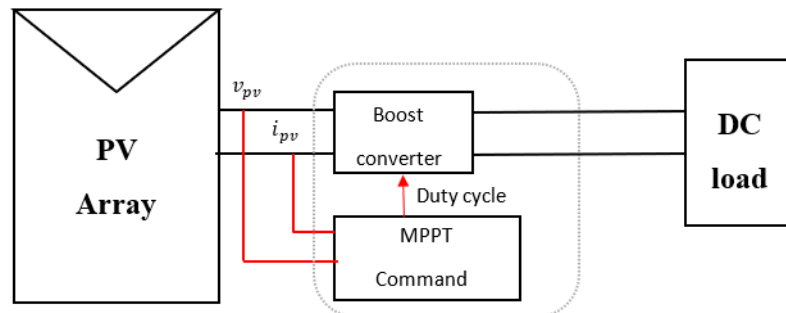
Figure 5.1: The off-grid System architecture.

Every time the system is kept the same and only the MPPT algorithm is changed in order to observe the influence on the different performances of the system. The figure 5.2 shows the proposed system structure using the P&O algorithm as example in MATLAB/SIMULINK platform.
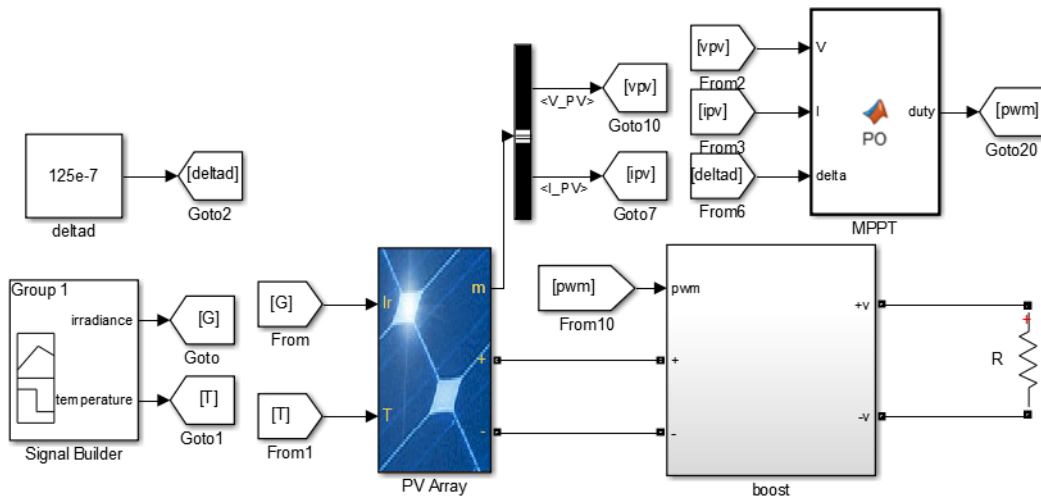
Figure 5.2: The off-grid System structure in MATLAB/SIMULINK.

The PV panel converts the energy that comes from the sun to electric energy. The modules can be connected to each other in series and/or parallel to form PV array. The specification of the PV array given in the table 5.1.

Module	Aavid Solar ASMS-220P
Maximum Power (W)	220.5
Cells per module (Ncell)	60
Open circuit voltage Voc (V)	36.8
Short-circuit current Isc (A)	8.08
Voltage at maximum power point Vmp (V)	30
Current at maximum power point Imp (A)	7.35
Temperature coefficient of Voc (%/deg.C)	-0.33641
Temperature coefficient of Isc (%/deg.C)	0.038465
Parallel strings	3
Series-connected modules per string	4

Table 5.1: The specification of the PV array.

In all the off-grid simulations the same Boost converter is used which controlled by varying the duty cycle through MPPT technique. So, controlling the output power. The characteristics of the boost used given in the table 5.2:

The input capacitor C_i	$3 * 10^{-5} F$
Inductance L	$2 * 10^{-3} H$
The output capacitor C_o	$5 * 10^{-4} F$
Switching frequency f_{sw}	5 kHZ
Resistance	72 ohms

Table 5.2: The characteristics of boost converter.

The figure 5.3 presents the boost converter structure used in the simulation.
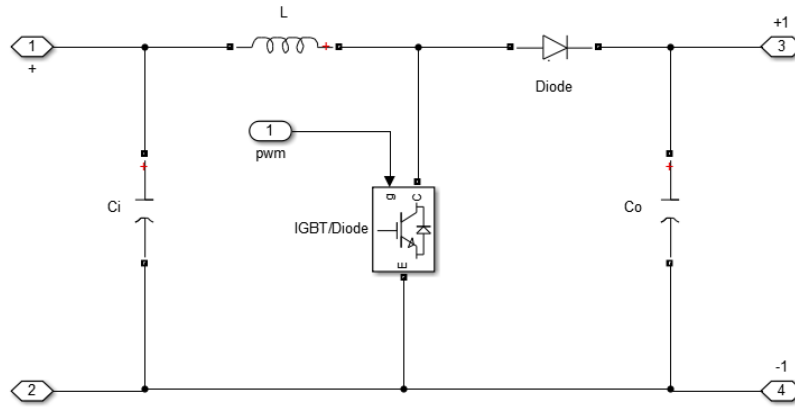
Figure 5.3: The boost converter structure.

The simulation results for the MPPT algorithms has been established under different conditions to see the response of each one. The table 5.3 presents the irradiance and temperature in function of time.

time (S)	0-1	1-2	2-3	3-4	4-5
Irradiance (W/m^2)	1000	1100	800	400	700
Temperature (C°)	25	45	35	5	33

Table 5.3: The variation of the environmental conditions.

As mentioned previously the network must be trained before used. So, the proposed multi layer Neural Network algorithm is trained by using "nntool" in MATLAB. The feed-forward network with a back-propagation algorithm assures the adjusting of weights which is determined at the offline training.

The characteristics of the network shown in the table 5.4.

Type of network	Feed-forward
Hidden Layer activation function	Sigmoid
Output Layer activation function	Linear
Back-propagation algorithm	Levenberg-Marquardt
Performance	Mean Squared Error (MSE)
Number of hidden neurons	5
Number of samples	625

Table 5.4: The characteristics of the network.

The samples are obtained by varying the temperature from 5 °C to 45 °C and irradiance from 100 W/m^2 to 1100 W/m^2. Some data is used to test and validate the network after training.

The figure 5.4 presents a small Mean Squared Error (MSE), i.e, the network is well trained, the best MSE obtained is $4.2046*10^{-5}$ at epoch 77. Also, the convergence of the training, validating ,testing samples.
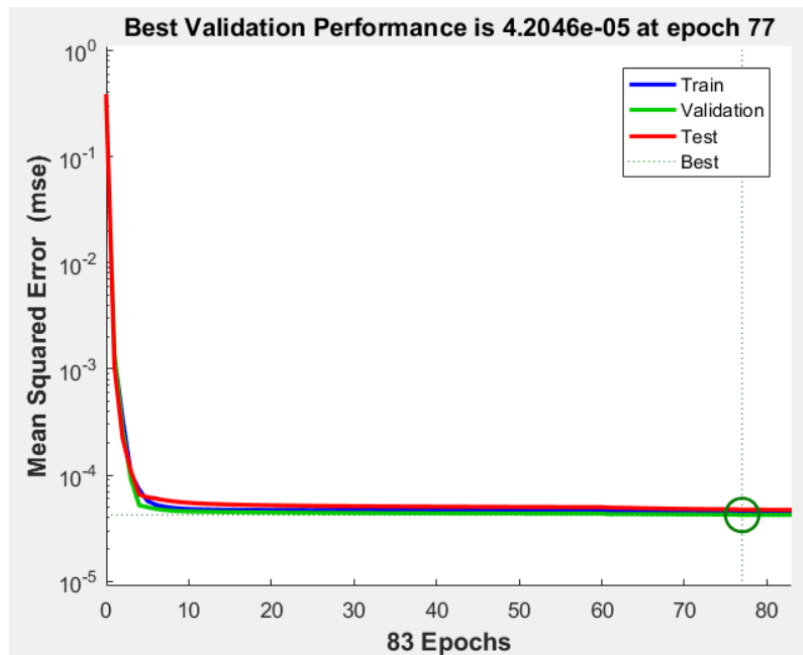
Figure 5.4: The Mean Squared Error (MSE) of the network.

The figure 5.5 shows that the data fall along a 45 degree line (R = 0.99 ≈ 1). Where, the network outputs are equal to the targets.
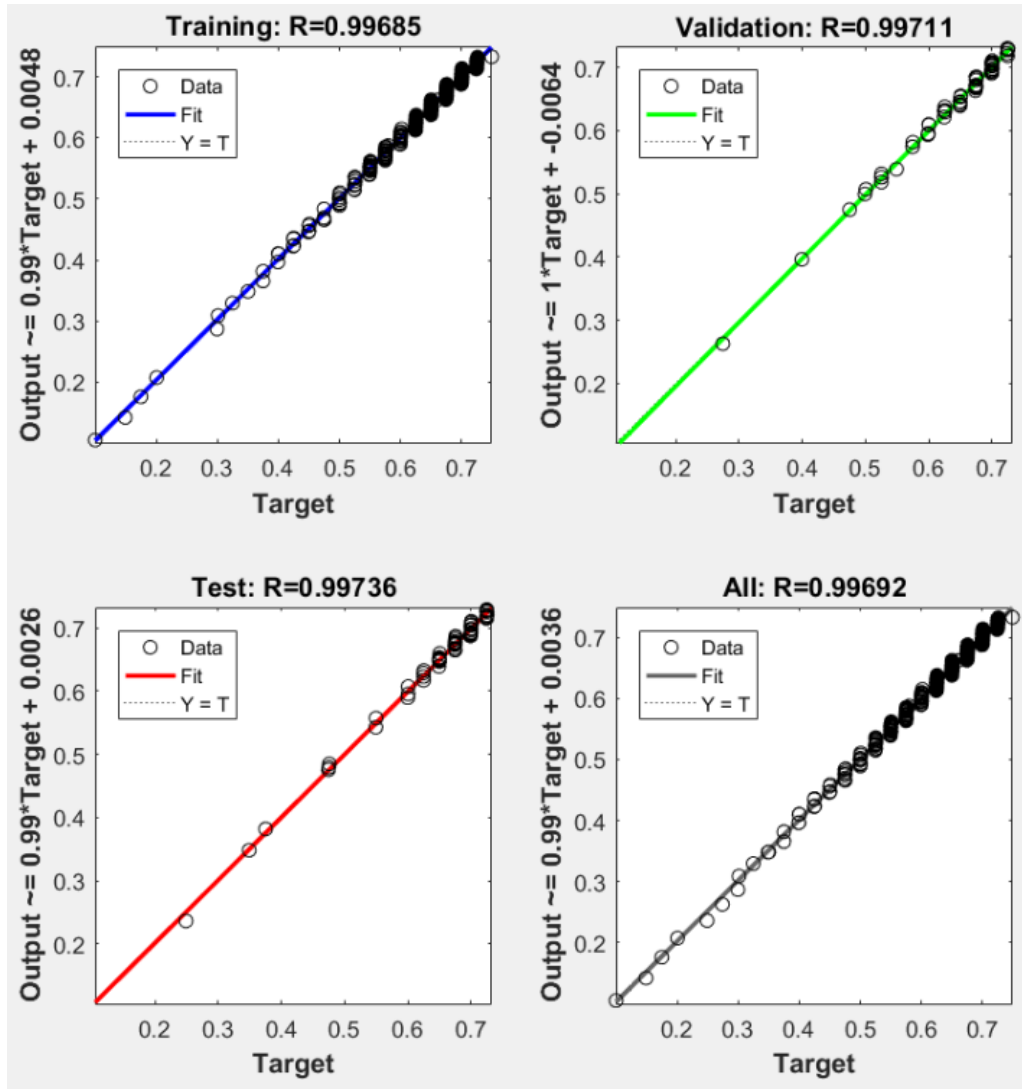
Figure 5.5: The targets convergence.

It is observed from the figure 5.5 that all the samples are aligned on the same line which represent a high accuracy of the acquisition of data and the validity of them.

The four MPPT algorithms are plotted in the same figure in order to compare them and to see the behaviour of each algorithm in a different temperatures and irradiances especially in the fast changing. The meteorologic conditions used are shown in the table 5.3.

The figure 5.6 shows the output power consumed by the load using the four MPPT algorithms.
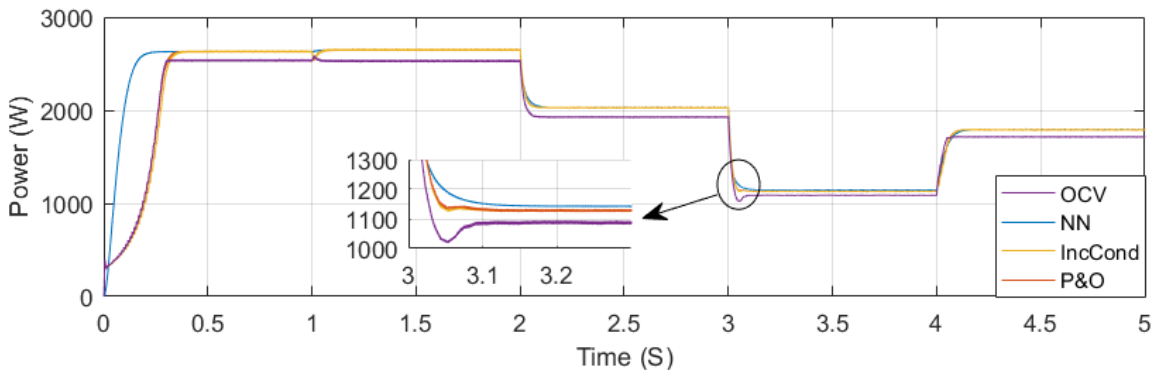
Figure 5.6: The output power of the different MPPT algorithms.

The figure 5.7 presents the voltage over the load with the different MPPT algorithms.
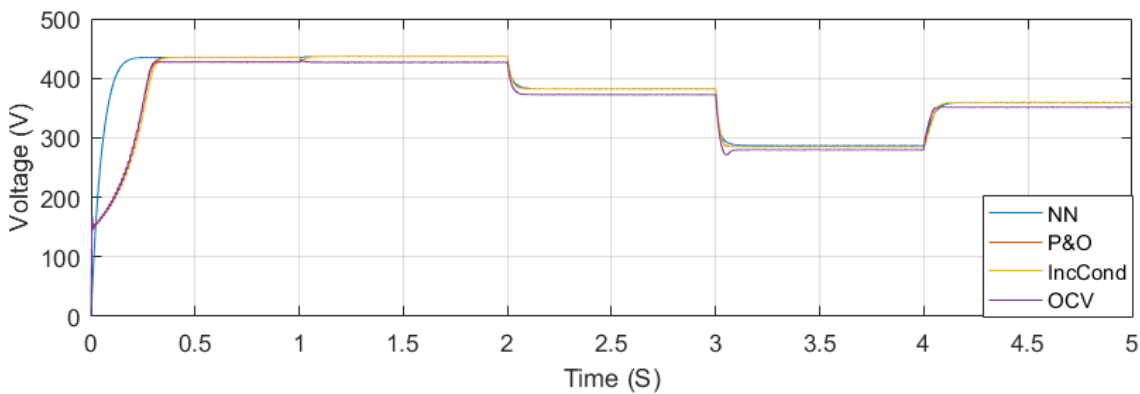
Figure 5.7: The output voltage of the different MPPT algorithms.

The figure 5.8 indicates the duty cycle of the different MPPT algorithms.
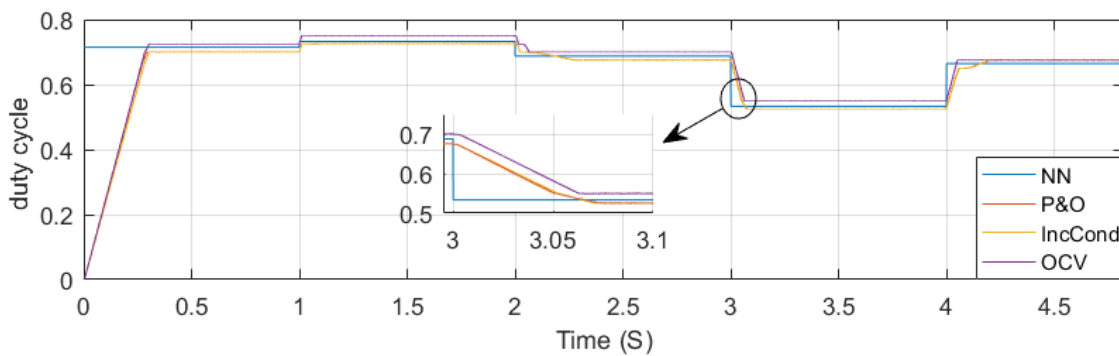
Figure 5.8: The duty cycle of the different MPPT algorithms.

According to the figure 5.6, 5.7 and 5.8 the NN algorithm has quick response, i.e, it requires less time to reach the MPP and high efficiency and less oscillation comparing with the conventional methods. The OCV has also relatively short response time comparing with *P&O* and IncCond but less output power. *P&O* has a high output power but, presents an oscillation around MPP. Also, IncCond has high output power but takes more time to reach the MPP.

In the rapidly changing of irradiance *P&O*, OCV, and IncCond present an overshoot. After that, both of *P&O* and IncCond stabilize in MPP. However, OCV converges far from maximum power point.

The figure 5.8 shows that the NN reached immediately the corespondent duty cycle during the variation of temperature or irradiance.

The main Disadvantages of NN algorithm are:

The NN needs a well training with a huge samples to achieve a good results.
Any modification of the system will leads a new training of the Neural Network.

5.2   On-grid system

All the performances, characteristics and obtained results are highlighted in the next sections.

5.2.1   The system's structure

The single-phase two-stage photovoltaic grid-connected system used is modeling as the following. A PV array with capacity of 2341 W in standard test conditions (STC) is connected to a boost converter which controlled through an MPPT algorithm. A dc link capacitor is introduced between the boost converter and the inverter to get a constant dc link voltage. An output L filter is connected to the utility grid to reduce the harmonics around the switching frequency. A signal builder assures the variation of irradiance and temperature as presented previously in the table 5.3.

The global diagram of the system is shown in the figure 5.9.
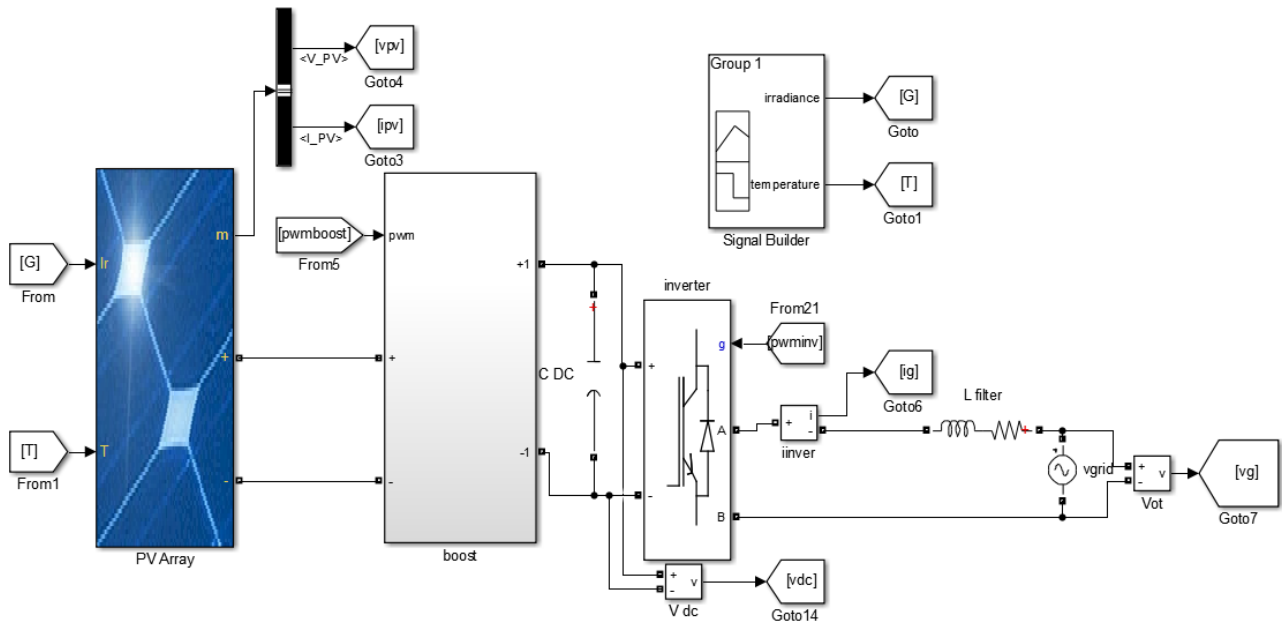
Figure 5.9: The on-grid system structure.

5.2.2   The system's parameters

In this part of the results we have take another components comparing with the first part, their characteristics are presented as follows:

The table 5.5 presents the parameters of the PV array used.

Module	Suntech Power STP195-24-Ad
Maximum Power (W)	195.078
Cells per module (Ncell)	72
Open circuit voltage Voc (V)	45.4
Short-circuit current Isc (A)	5.69
Voltage at maximum power point Vmp (V)	36.6
Current at maximum power point Imp (A)	5.33
Temperature coefficient of Voc (%/deg.C)	-0.32599
Temperature coefficient of Isc (%/deg.C)	0.034007
Parallel strings	3
Series-connected modules per string	4

Table 5.5: The specification of the PV array.

The other component's parameters are given in the table 5.6.

The input capacitor C_i	$5*10^{-5}F$
Inductance L	$3*10^{-2}H$
Switching frequency f_{sw}	5 kHZ
The dc link capacitor C_{dc}	$12*10^{-3}F$
The dc link voltage V_{dc}	$400V$
The grid frequency f	50 HZ
The utility grid voltage V_g	$220V_{rms}$
The output L filter L_f	$10*10^{-3}H$
The output L filter resistance R_f	0.1 Ω

Table 5.6: The characteristics of the system.

5.2.3   Design of the components

As mentioned before in 3.3.1 the inductance value of the boost converter is designed based on the equation 3.10 So, the chosen inductance value is L= $3*10^{-2}H$.

The sizing of the dc link capacitor has been established based on the rated power of the system and the equation 3.25.
As a result, C_{dc}=$12*10^{-3}F$.

The sizing of the output L filter is done based on the equation 3.13. So consequently, $L_f = 10*10^{-3}H$.

5.2.4   The simulation results and discussion

The platform MATLAB/SIMULINK is used to simulate the single phase two stage photovoltaic grid connected in which the control of the dc link voltage, the injected current and MPP are achieved. Also, the influence of variation in the climatic conditions on the output performance of the system. After that, the different MPPT algorithms explained in this thesis previously are simulated and discussed.

To present the performance of the different system output an efficient MPPT algorithm is needed, for this reason a modified-Neural Network MPPT algorithm is proposed. In the first part of the simulation the system works in STC using the modified-Neural Network as an MPPT algorithm which has like inputs the solar irradiance and temperature and the PV array voltage reference represents the output.

The chosen NN algorithm is a multilayer feed-forward network with back propagation algorithm in order to adjust the weights and obtained a small mean squared error (MSE). The figure 5.10 indicates it's structure.
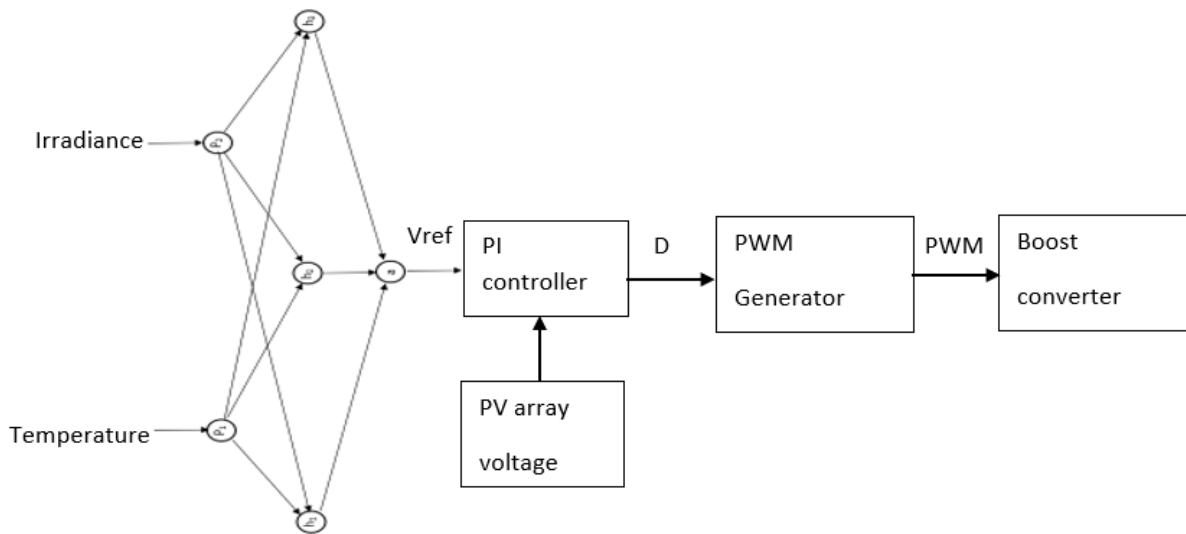
Figure 5.10: The schematic of the modified-Neural Network algorithm.

The inverter controller contains two loops, the first one controls the dc link voltage using a PI controller which compares the real dc link voltage to a reference value. The output of this loop is the maximum value of the reference current. The PLL gives the grid voltage phase. A sinusoidal signal is generated and synchronized with the grid voltage phase and multiplied by the maximum value of the reference current which gives the reference current. The second loop makes the injected current follow the reference current using Pr controller. The Pr controller generates the reference signal to the PWM generator to control the inverter's switches. The figure 5.11 shows the inverter controller block.
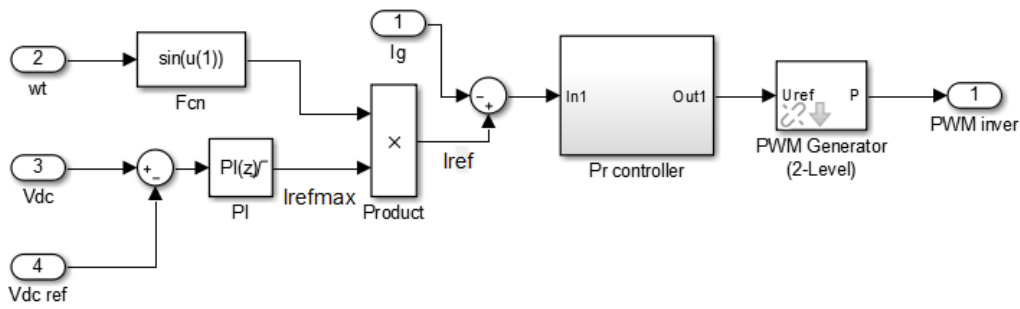
Figure 5.11: The inverter controller block diagram.

Using the equation 3.25 and the characteristics in the table 5.6, the dc link voltage ripple equal to: Δv_{dc}= 1.55V.

The figure 5.12 presents that the dc link voltage is following the reference voltage ($V_{dcref} = 400V$) with a peak to peak voltage ripple of Δv_{dc}= 1.50V, this value represents 0.375% of the reference value and as it seems it's very close to the theoretic value (1.55V).
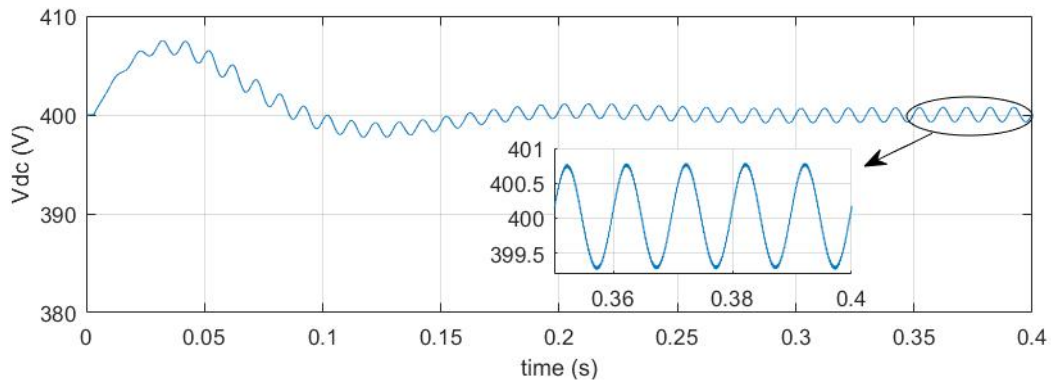
Figure 5.12: The dc link voltage.

The figure 5.13 shows the connection between the inverter and the utility grid in which the injected current transformed to sinusoidal form.
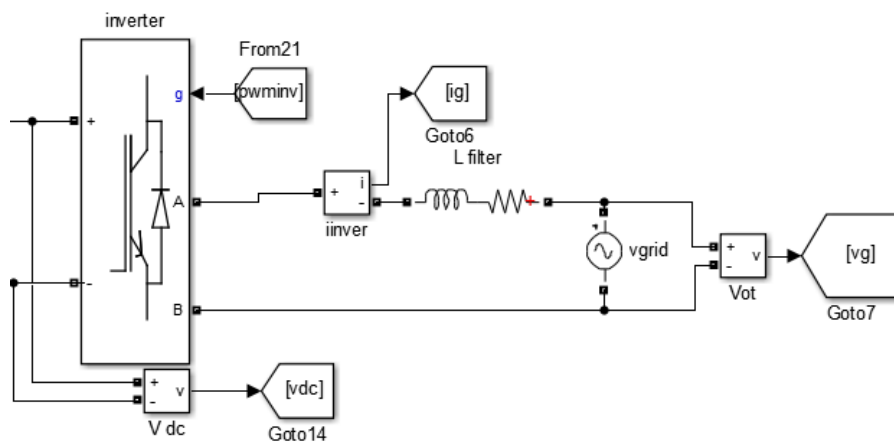
Figure 5.13: The inverter-grid connection.

The figure 5.14 shows that the injected current and the grid voltage are in phase and sinusoidal what means a unity power factor is achieved. So then, the validation of the current control loop.
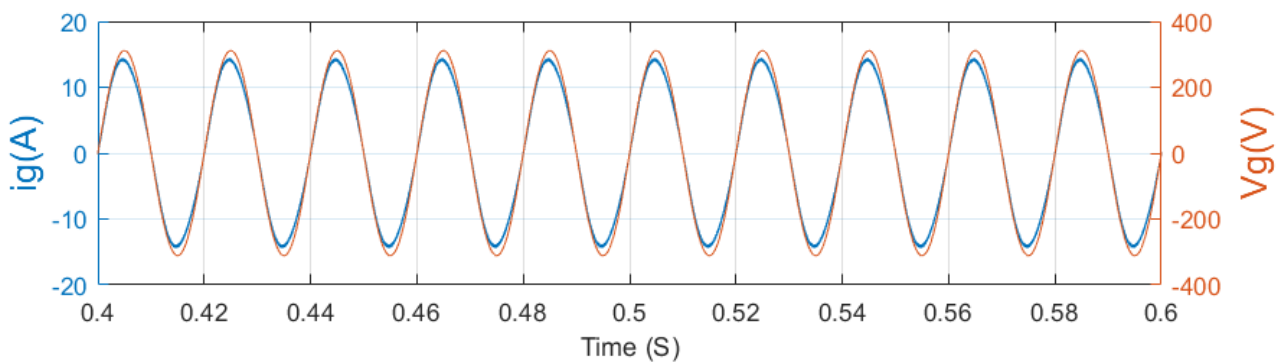
Figure 5.14: The grid voltage and the injected current.

Additionally, in the figure 5.15 a THD of 2.96% < 5% is achieved. Consequently, the condition mentioned in the section 3.11 is satisfied and the utility of output L filter is reached.

Fundamental (50Hz) = 14.09 , THD= 2.96%
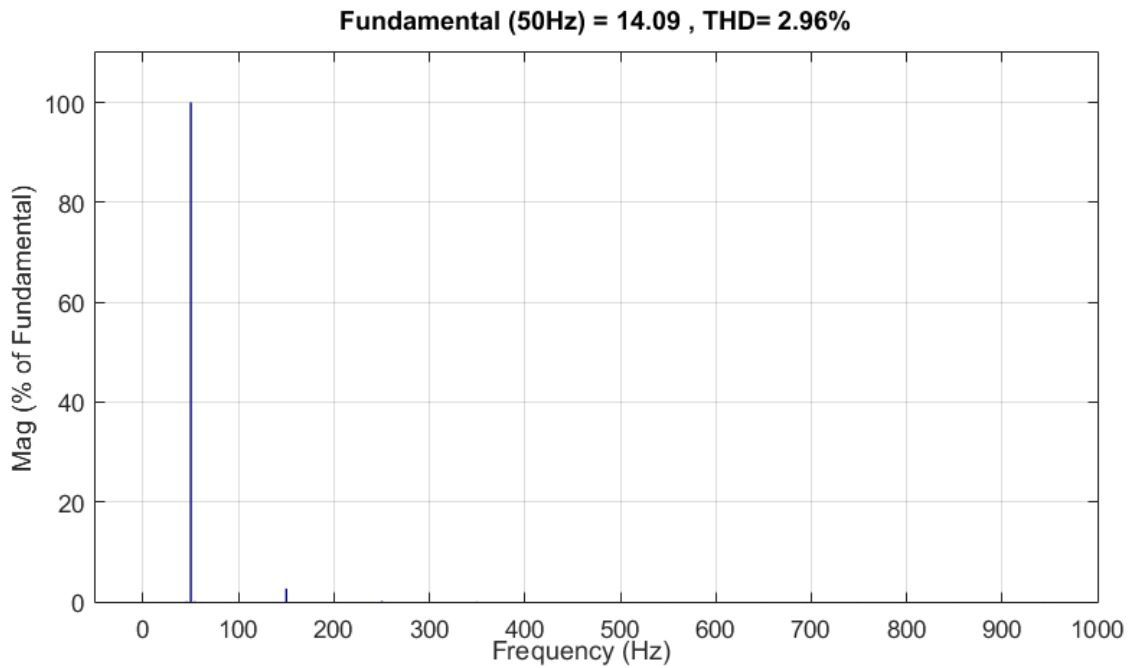
Figure 5.15: Total Harmonic Distortion.

The figure 5.16 indicates the extracted power from the PV array in the STC condition using the modified-Neural Network technique.
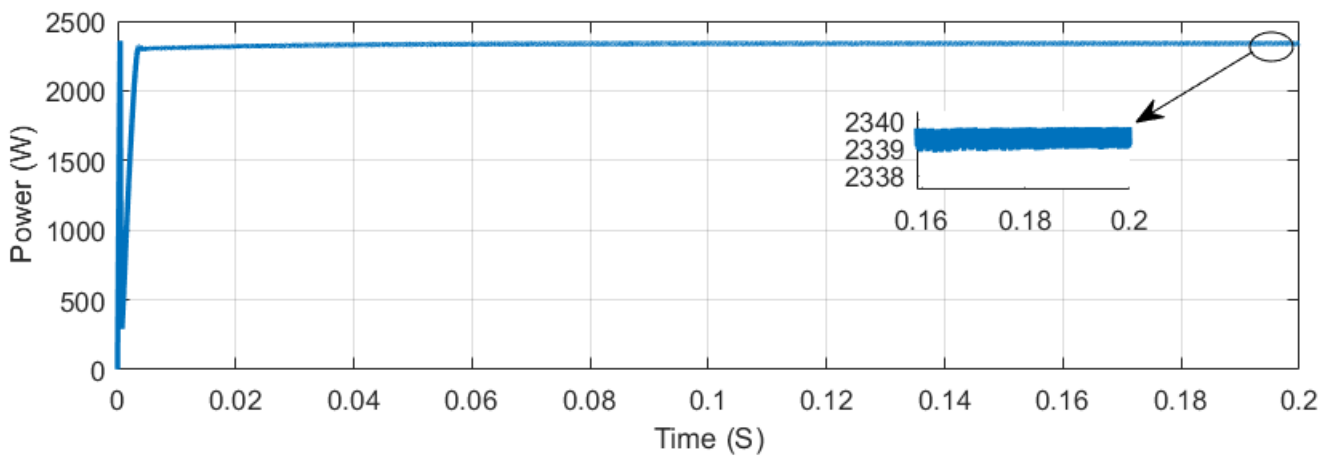
Figure 5.16: The extracted PV array power using the modified-Neural network technique.

As it seems form the figure 5.16 the modified-Neural Network algorithm presents a fast response with a 0.12 s as response time, with a high accuracy as 99.93% from the maximum PV array power.

The figure 5.17 shows the active power injected in the grid.
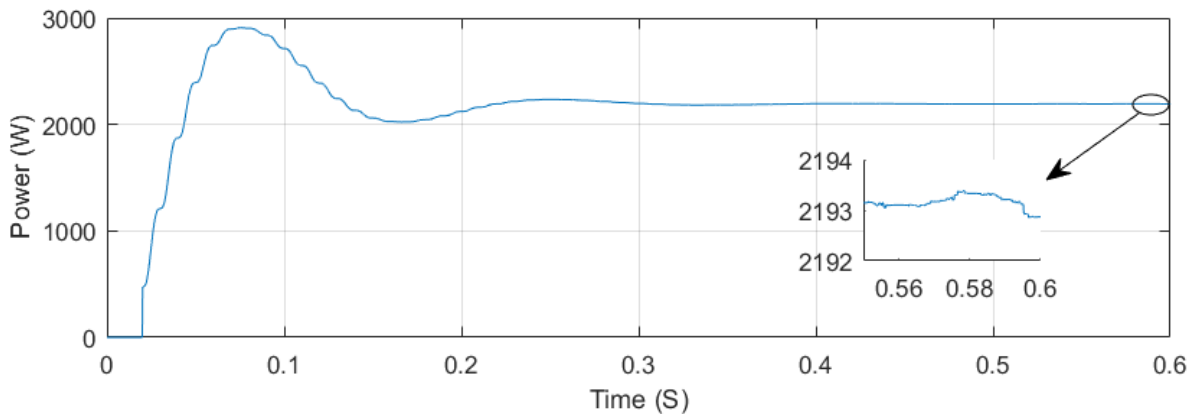
Figure 5.17: The active power injected in the grid.

As indicated in the figure 5.17 a power of 2193 W is injected which represents 93.68% from the maximum PV array power and 93.73% from The extracted PV array power using the modified-Neural Network algorithm.

5.2.5   Comparison of Different MPPT Algorithms

In order to prove the efficiency of the modified-NN algorithm and showing the difference between the modified-NN and the NN algorithm (duty cycle as output) a simulation of the on-grid system as presented in figure 5.9 is made.
The figure 5.18 shows the extracted power from the PV array using both of NN algorithms.
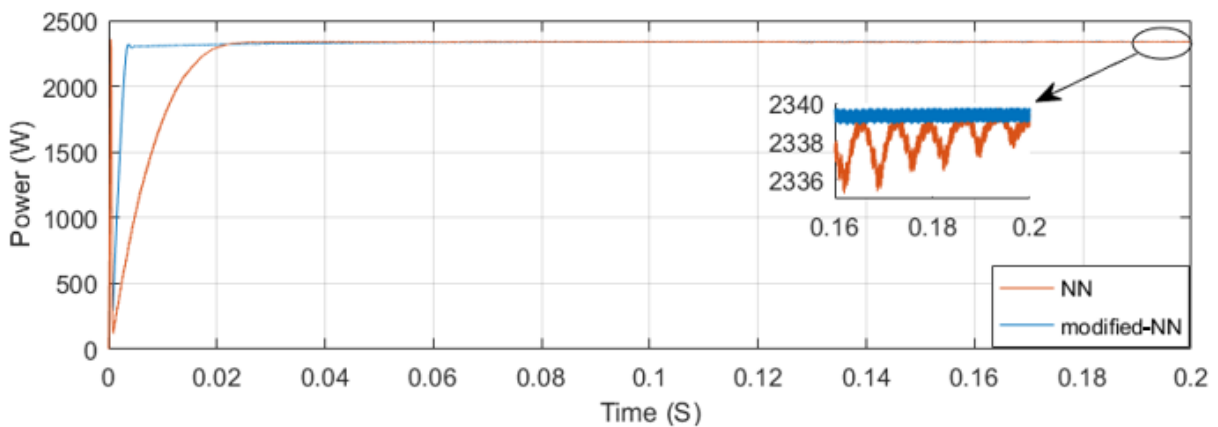
Figure 5.18: The extracted power from the PV array using both of NN algorithms.

It is observed from the figure 5.18 that the modified-NN is more efficient than the classic Neural Network by a high precision and stability. While, $(\Delta P = 2339.8 - 2339 = 0.8W)$ for the modified-NN and $(\Delta P = 2339.6 - 2335.4 = 4.2W)$ for the NN. But, this later is more quick than the modified-NN by a response time of 0.07 s and 0.12 s for the modified-NN. The delay that presents in the modified-NN due to the time taken by PI controller to converge.

The main difference between the two Neural networks algorithms is that the modified NN has a constant reference voltage with a variable duty cycle. On the contrary, the NN has a constant duty cycle with a variable voltage.

As shown in figure 5.12 an oscillation around the dc link voltage with 1.5V peak to peak voltage ripple which represents the output voltage of the boost converter. So, using the equation 3.8 it is clear that in the presence of the output voltage ripple and for making the PV array works in the optimum point voltage a variable duty cycle must be presented that's what is used in the modified-NN technique as shown in the figure 5.19.
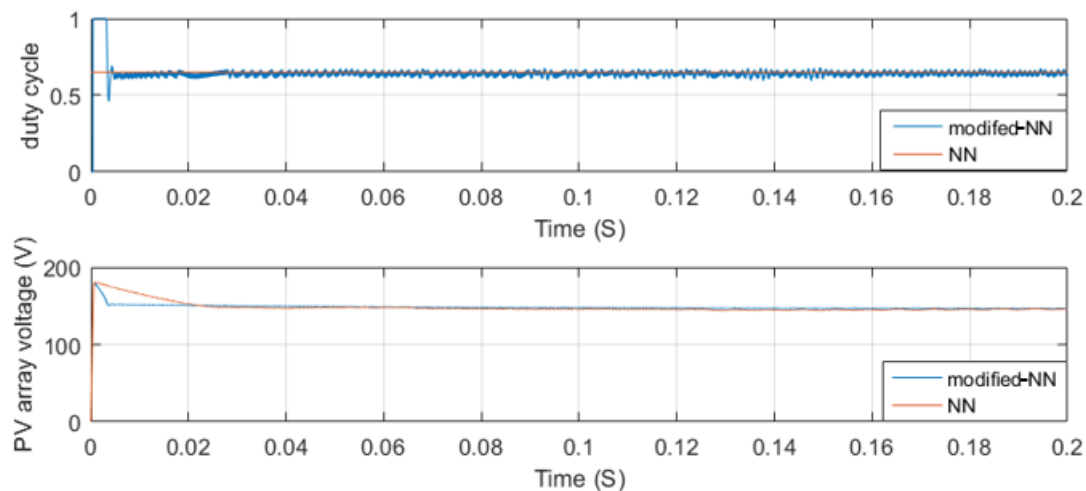
Figure 5.19: The PV array voltage and duty cycle using both of NN algorithms.

To see the influence of the variation in the climatic conditions on the output performance of the system, different couples of irradiance and temperature are presented as shown in the table 5.7.

time (S)	0-1	1-2	2-3	3-4	4-5	5-6
Irradiance (W/m^2)	1000	1100	800	1000	850	400
Temperature (C°)	25	25	15	45	31	5

Table 5.7: The variation of the environmental conditions.

The figure 5.20 illustrates from top to bottom the extracted power from the PV array and the injected active power in the grid. The subsystem (boost + inverter) has high efficiency with $\eta = 93.15\%$ between 1-2 and $\eta = 97.27\%$ between 5-6. So with the rising of irradiance both of PV power and losses increase. Between 0-1 and 3-4 the irradiance is constant and the temperature varies. Consequently, as observed the augmentation of temperature has a negative influence on the power. On the other hand, between 0-1 and 1-2 the temperature is constant and the irradiance varies so then, the augmentation of irradiance leads an increasing of power. Following this, the best power is obtained when the irradiance is maximal and temperature is minimal.
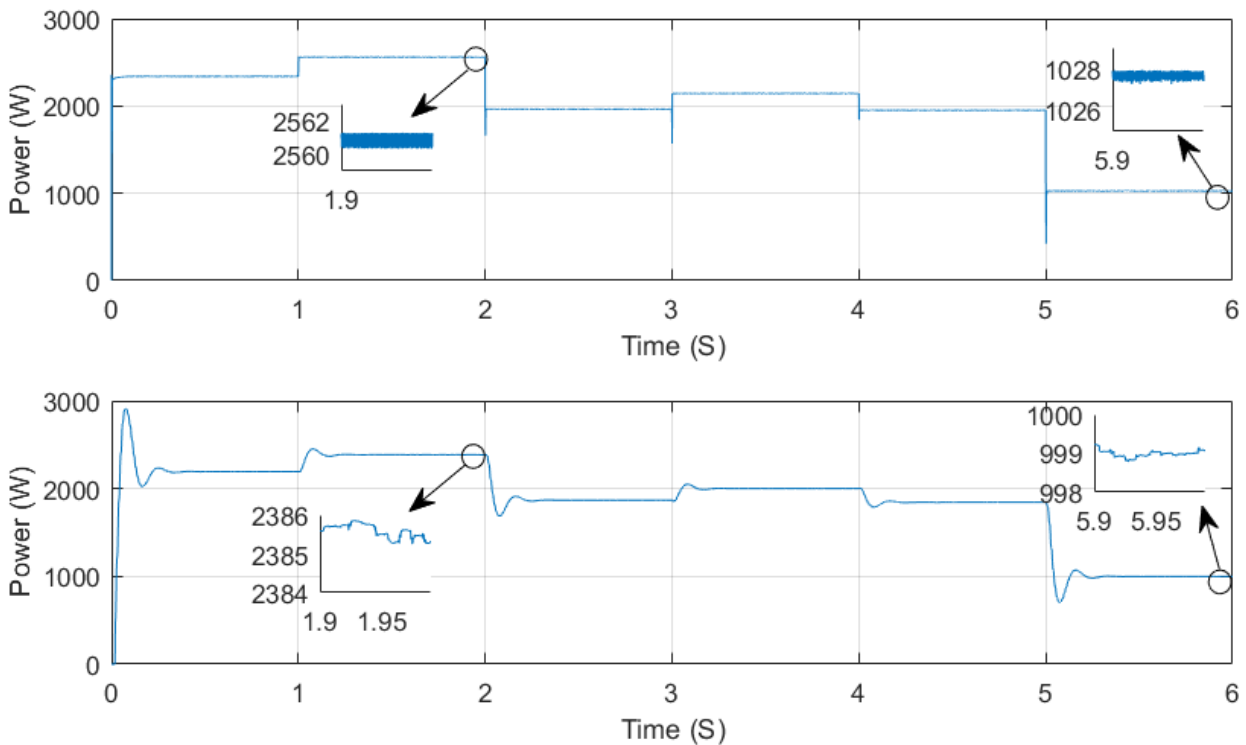
Figure 5.20: The extracted power from PV array and the active power injected.

The figure 5.21 presents from bottom to top Total Harmonic Distortion (THD) and the dc link voltage. It can be noticed that in the preferable meteorological conditions (high irradiance and low temperature) the voltage ripple is high and THD is small. On the other hand, in high temperature and low irradiance the voltage ripple is small and THD is high.
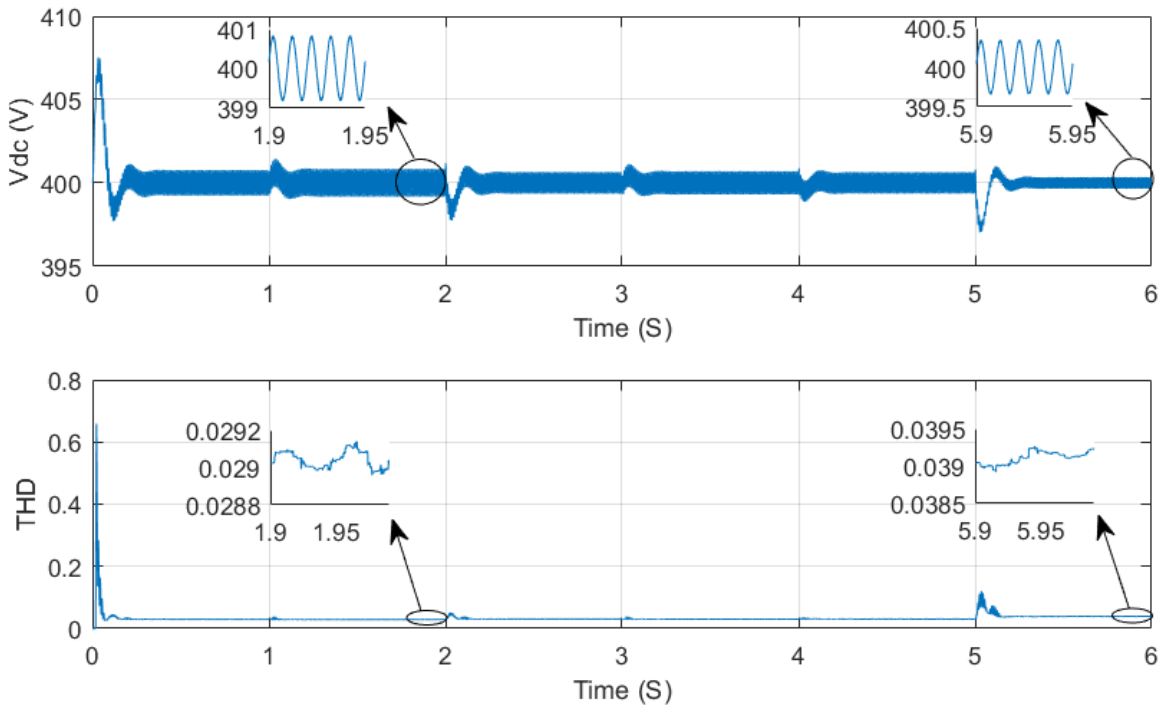
Figure 5.21: The dc link voltage and THD.

The figure 5.22 indicates the extracted power using modified NN, NN, P&O, IcnCond and OCV algorithms under STC conditions. The NN algorithms present a fast response ($t_r = 0.07\ s$ for NN and $t_r = 0.12\ s$ for modified-NN) following by OCV method with $t_r = 0.31\ s$ after that, we have P&O with $t_r = 0.32S$ and finally, IncCond with $t_r = 0.35\ s$.

In steady state, All the algorithms track the maximum power except the OCV which has a high error. The OCV has the highest oscillation and it's far from the theoretical maximum power. Comparing with OCV method, both of P&O and IcnCond have less oscillation around MPP. NN technique presents small oscillation comparing with the conventional methods. The smoothest response is reached by the modified-NN. The modified-NN achieves the better results, obtaining a tracking performance of 99.93%.
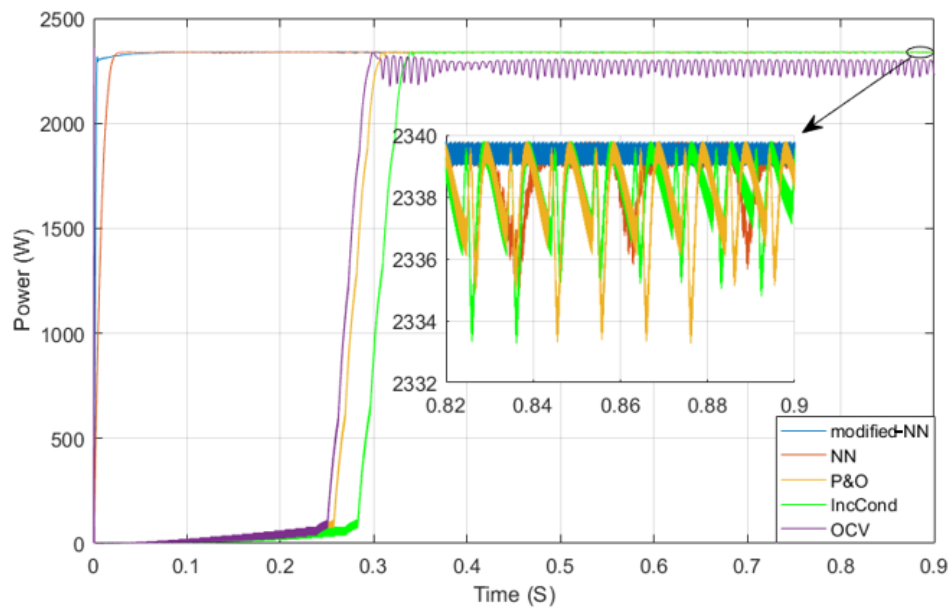
Figure 5.22: The extracted power from PV array using different MPPT algorithms.

To see the behavior of the MPPT algorithms under different climatic conditions as have done in the off-grid system, the system is simulated in different irradiances and temperatures as indicates in table 5.7. The figure 5.23 shows The extracted power from PV array using different MPPT algorithms under different environmental conditions.
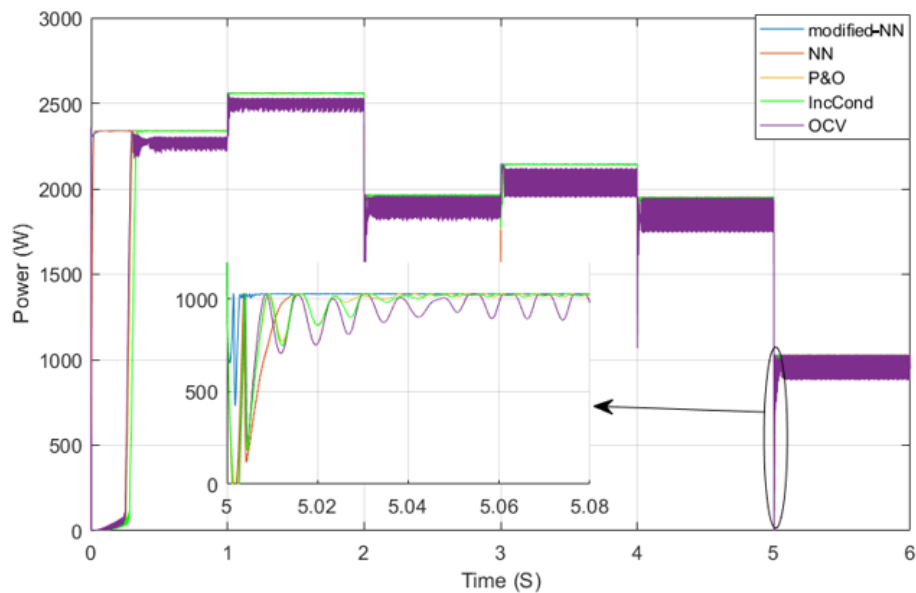
Figure 5.23: The extracted power from PV array using different MPPT algorithms under different environmental conditions.

As it seems with the increasing of irradiance and decreasing of temperature the extracted power increases. In the rapidly changing of climatic conditions the OCV method presents the highest overshoot and oscillation. Also, the other algorithms have an overshoot but, less than OCV. After that, they converge to MPP. The smallest overshoot is reached by the modified-NN.

Chapter 6

Conclusion and perspectives

6.1   General conclusions

The work presented in this thesis consists the study of the MPPT algorithms to improve the efficiency of an off-grid system and on grid0system. The PV system contains a lot of components, the most important is the PV cell which converts the energy that comes from the sun into electricity. To understand it's functionality several models have been proposed as the "one-diode model", the"two-diode model", the "polynomial model. The output current and voltage of the PV cell depends on irradiance and temperature, for this reason, a study about the influence of irradiance and temperature on the PV cell was presented. To satisfy the industrial energy needs a combination in series and/or parallel can be done to get a PVG. This one needs a protection which represents bypass diode and blocking diode.

The PVG cell has many operating points depending on the intersection between the load characteristic and PV characteristic. So, the direct PVG-load connection is not efficient. To make the system works in MPP, a power stage is introduced between the source and the load like a boost converter which is explained in detail in the third chapter. This one is controlled through an MPPT algorithm. Subsequently, various techniques for the pursuit of PPM existing in the literature were mentioned. For each of them, the advantages and disadvantages are presented. The P&O and IncCond algorithms are widely used in previous research. The integration of inverter is used in case of ac load or for the grid connection. In the latter case we distinguish the three phase connection and the single phase connection which also divided in single stage inverter and two stage inverter. The last structure presents more flexibility than the single stage inverter. To connect the the inverter with the grid it's necessary to synchronized both of them which is achieved via the PLL. A low-pass filter is introduced between the inverter and the grid to enhance the quality of the injected power.

In the fourth chapter the Neural Networks theory has been presented starting by the definition, the neural model, network architectures, Neural Network design steps, the Mean Squared Error and the back-propagation algorithm. To integrate the Neural Network as an MPPT algorithm it's necessary to follow the next steps: data collection, selection of network structure, training the network and finally testing the network before used.

In order to see the features of each MPPT algorithm and make a comparison between them an off-grid system has been simulated firstly using the MATLAB/SIMULINK platform. All the MPPT algorithms control the boost converter by the variation of duty cycle. All of NN, P&O, OCV and IncCond track MPP by different efficiency and accuracy. The highest efficiency and the faster response are obtained by the NN algorithm. The OCV has also relatively short response time comparing with P&O and IncCond but less output power. In case of fast changing of meteorological conditions the conventional MPPT techniques present an overshoot. The NN reached immediately the corespondent duty cycle during the variation of temperature or irradiance.

Secondly, the single-phase two-stage photovoltaic grid-connected system is simulated. This later controls the MPP, the dc link voltage and the injected current. All the components are designed to have a good performances. Comparing with the off-grid system we have simulated another MPPT algorithm based on NN which achieved a high tracking. A small dc link voltage ripple is reached which leads to get an acceptable THD. The injected current is synchronized with the utility grid voltage. As result, high power quality has been established. Comparing the two NN mppt algorithms the modified-NN is more efficient than the classic Neural Network method by a high precision and stability. However, the classic NN is more quicker than the modified-NN due to the presence of PI controller. To establish the influence of the variation in the climatic conditions on the output performance of the system we make a variation of irradiance and temperature. Consequently, with the rising of irradiance both of PV power and losses increase, the augmentation of temperature has a negative influence on the power and the augmentation of irradiance leads an increasing of power. So then, the best power is obtained when the irradiance is maximal and temperature is minimal. As noticed in the high irradiance and low temperature high voltage ripple and small THD are presented. Contrary, in high temperature and low irradiance the voltage ripple is small and THD is high .

For the MPPT algorithms,a simulation of the modified-NN, NN, P&O, IncCond and OCV has been established. As a result, the NN algorithms present a fast response following by OCV method, after that, P&O and finally, IncCond. In steady state, All the algorithms track the maximum power except the OCV which has a high error. The OCV has the highest oscillation and it's far from the theoretical maximum power. Comparing with OCV method, both of PO and IcnCond have less oscillation around MPP. NN technique presents small oscillation comparing with the conventional methods. The smoothest response is reached by the modified-NN. In the rapidly changing of climatic conditions the OCV method presents the highest

overshoot and oscillation. Also, the other algorithms have an overshoot but less than OCV. After that, they converge to MPP. The smallest overshoot is reached by the modified-NN.

6.2   Future perspectives

The implementation of all the MPPT algorithms presented previously in the hardware and make the validation of the NN algorithms their performances.

Equipped both of the off-grid and on-grid system by a solar tracking system to increase the absorbed power by the PV array.

Bibliography

[1] S.ABOUDA, *Contribution a la commande des systemes photovoltaiques: application aux systemes de pompage.* PhD thesis, the national engineering school of SFAX, the national engineering school of SFAX, 2015.

[2] M. R. Rashel, *Modeling photovoltaic panels under variable internal and environmental conditions with non-constant load.* PhD thesis, the university of Évora, 2018.

[3] P. D. Kale and D. Chaudhari, "A review on maximum power point tracking (mppt) controlling methods for a photovoltaic system," *International Journal of Emerging Science and Engineering (IJESE)*, vol. 1, no. 5, 2013.

[4] A.Saliha, "Modélisation et commande d'un système de pompage photovoltaïque." magister thesis university « FERHAT ABBAS » ALGERIA, 2014.

[5] Y. hameed khattak, *Modeling of High Power Conversion Efficiency Thin Film Solar Cells.* PhD thesis, university polytechnic of valancia, 2019.

[6] S. petibon, *Nouvelles architectures distribuées de gestion et de conversion de l'énergie pour les applications photovoltaïques.* PhD thesis, University Toulouse 3 Paul Sabatier , France.., 2009.

[7] K. Zweibel, *Basic photovoltaic principles and methods.* February 1982.

[8] O. Gergaud, B. Multon, and H. B. Ahmed, "Analysis and experimental validation of various photovoltaic system models," 2002.

[9] M. Azab, "A new maximum power point tracking for photovoltaic systems," *WASET. ORG*, vol. 34, pp. 571–574, 2008.

[10] A.D.Hansen, P. E.Sørensen, L. H.Hansen, and H.W.Bindner, *Models for a stand-alone PV system.* Forskningscenter, 2001, 1219 (EN).

[11] A.bELKAID, *Conception et implémentation d'une commande MPPT de haute performance pour une chaine de conversion photovoltaïque autonome.* PhD thesis, university of FERHAT ABBAS SETIF 1, Algeria, 2015.

[12] I. A. M. A. Hossan, *Solar power as renewable energy for home systems in bangladesh.* Department of Electrical Electronic Engineering Northern University Bangladesh, 2014.

[13] J. Khanam and S. Y. Foo, "Neural networks technique for maximum power point tracking of photovoltaic array," in *SoutheastCon 2018*, pp. 1–4, IEEE, 2018.

[14] J. Li and H. Wang, "A novel stand-alone pv generation system based on variable step size inc mppt and svpwm control," in *2009 IEEE 6th International Power Electronics and Motion Control Conference*, pp. 2155–2160, IEEE, 2009.

[15] L. Jie and C. Ziran, "Research on the mppt algorithms of photovoltaic system based on pv neural network," in *2011 Chinese Control and Decision Conference (CCDC)*, pp. 1851–1854, IEEE, 2011.

[16] C.-Y. Won, D.-H. Kim, S.-C. Kim, W.-S. Kim, and H.-S. Kim, "A new maximum power point tracker of photovoltaic arrays using fuzzy controller," in *Proceedings of 1994 Power Electronics Specialist Conference-PESC'94*, vol. 1, pp. 396–403, IEEE, 1994.

[17] A. A. Kulaksız and R. Akkaya, "A genetic algorithm optimized ann-based mppt algorithm for a stand-alone pv system with induction motor drive," *Solar Energy*, vol. 86, no. 9, pp. 2366–2375, 2012.

[18] L. Bouselham, M. Hajji, B. Hajji, and H. Bouali, "A new mppt-based ann for photovoltaic system under partial shading conditions," *Energy Procedia*, vol. 111, pp. 924–933, 2017.

[19] J. Khanam and S. Y. Foo, "Neural networks technique for maximum power point tracking of photovoltaic array," in *SoutheastCon 2018*, pp. 1–4, IEEE, 2018.

[20] A. Harrag, S. Messalti, and Y. Daili, "Innovative single sensor neural network pv mppt," in *2019 6th International Conference on Control, Decision and Information Technologies (CoDIT)*, pp. 1895–1899, IEEE, 2019.

[21] M. D. Singh, V. Shine, and V. Janamala, "Application of artificial neural networks in optimizing mppt control for standalone solar pv system," in *2014 International Conference on Contemporary Computing and Informatics (IC3I)*, pp. 162–166, IEEE, 2014.

[22] M. Arjun and J. Zubin, "Artificial neural network based hybrid mppt for photovoltaic modules," in *2018 International CET Conference on Control, Communication, and Computing (IC4)*, pp. 140–145, IEEE, 2018.

[23] E. Karatepe, T. Hiyama, *et al.*, "Artificial neural network-polar coordinated fuzzy controller based maximum power point tracking control under partially shaded conditions," *IET Renewable Power Generation*, vol. 3, no. 2, pp. 239–253, 2009.

[24] S. Motahhir, A. El Hammoumi, and A. El Ghzizal, "The most used mppt algorithms: Review and the suitable low-cost embedded board for each algorithm," *Journal of cleaner production*, vol. 246, p. 118983, 2020.

[25] A. Y. Mohammed, F. I. Mohammed, and M. Y. Ibrahim, "Grid connected photovoltaic system," in *2017 International Conference on Communication, Control, Computing and Electronics Engineering (ICCCCEE)*, pp. 1–5, IEEE, 2017.

[26] R. Ayop and C. W. Tan, "Design of boost converter based on maximum power point resistance for photovoltaic applications," *Solar Energy*, vol. 160, pp. 322–335, 2018.

[27] A. Yafaoui, B. Wu, and R. Cheung, "Implementation of maximum power point tracking algorithm for residential photovoltaic systems," in *2nd Canadian solar buildings conference Calgary*, pp. 10–14, Citeseer, 2007.

[28] M. A. G. De Brito, L. Galotto, L. P. Sampaio, G. d. A. e Melo, and C. A. Canesin, "Evaluation of the main mppt techniques for photovoltaic applications," *IEEE transactions on industrial electronics*, vol. 60, no. 3, pp. 1156–1167, 2012.

[29] M. Hlaili and H. Mechergui, "Comparison of different mppt algorithms with a proposed one using a power estimator for grid connected pv systems," *international journal of photoenergy*, vol. 2016, 2016.

[30] K. Hussein, I. Muta, T. Hoshino, and M. Osakada, "Maximum photovoltaic power tracking: an algorithm for rapidly changing atmospheric conditions," *IEE Proceedings-Generation, Transmission and Distribution*, vol. 142, no. 1, pp. 59–64, 1995.

[31] S. Samerchur, S. Premrudeepreechacharn, Y. Kumsuwun, and K. Higuchi, "Power control of single-phase voltage source inverter for grid-connected photovoltaic systems," in *2011 IEEE/PES Power Systems Conference and Exposition*, pp. 1–6, IEEE, 2011.

[32] N. Abd Rahim, J. Selvaraj, *et al.*, "Hysteresis current control and sensorless mppt for grid-connected photovoltaic systems," in *2007 IEEE International Symposium on Industrial Electronics*, pp. 572–577, IEEE, 2007.

[33] H. Ribeiro, F. Silva, S. Pinto, and B. Borges, "Single stage inverter for pv applications with one cycle sampling technique in the mppt algorithm," in *2009 35th Annual Conference of IEEE Industrial Electronics*, pp. 842–849, IEEE, 2009.

[34] O. Abdel-Rahim, M. Orabi, and M. E. Ahmed, "High gain single-stage inverter for photovoltaic ac modules," in *2011 Twenty-Sixth Annual IEEE Applied Power Electronics Conference and Exposition (APEC)*, pp. 1961–1967, IEEE, 2011.

[35] A. Panda, M. Pathak, and S. Srivastava, "A single phase photovoltaic inverter control for grid connected system," *Sadhana*, vol. 41, no. 1, pp. 15–30, 2016.

[36] C. Picardi, D. Sgro, and G. Gioffre, "A simple and low-cost pll structure for single-phase grid-connected inverters," in *SPEEDAM 2010*, pp. 358–362, IEEE, 2010.

[37] H. Cha and T.-K. Vu, "Comparative analysis of low-pass output filter for single-phase grid-connected photovoltaic inverter," in *2010 Twenty-Fifth Annual IEEE Applied Power Electronics Conference and Exposition (APEC)*, pp. 1659–1665, IEEE, 2010.

[38] M. Azri and N. A. Rahim, "Design analysis of low-pass passive filter in single-phase grid-connected transformerless inverter," in *2011 IEEE Conference on Clean Energy and Technology (CET)*, pp. 348–353, IEEE, 2011.

[39] L. Malesani, P. Tenti, E. Gaio, and R. Piovan, "Improved current control technique of vsi pwm inverters with constant modulation frequency and extended voltage range," *IEEE Transactions on industry applications*, vol. 27, no. 2, pp. 365–369, 1991.

[40] S. Samerchur, S. Premrudeepreechacharn, Y. Kumsuwun, and K. Higuchi, "Power control of single-phase voltage source inverter for grid-connected photovoltaic systems," in *2011 IEEE/PES Power Systems Conference and Exposition*, pp. 1–6, IEEE, 2011.

[41] N. Abd Rahim, J. Selvaraj, *et al.*, "Hysteresis current control and sensorless mppt for grid-connected photovoltaic systems," in *2007 IEEE International Symposium on Industrial Electronics*, pp. 572–577, IEEE, 2007.

[42] M. Salem and Y. Atia, "Control scheme towards enhancing power quality and operational efficiency of single-phase two-stage grid-connected photovoltaic systems," *Journal of Electrical Systems and Information Technology*, vol. 2, no. 3, pp. 314–327, 2015.

[43] K. Zhou, Z. Qiu, and Y. Yang, "Current harmonics suppression of single-phase pwm rectifiers," in *2012 3rd IEEE International Symposium on Power Electronics for Distributed Generation Systems (PEDG)*, pp. 54–57, IEEE, 2012.

[44] P. T. Krein, R. S. Balog, and M. Mirjafari, "Minimum energy and capacitance requirements for single-phase inverters and rectifiers using a ripple port," *IEEE Transactions on Power Electronics*, vol. 27, no. 11, pp. 4690–4698, 2012.

[45] Y.-M. Chen, H.-C. Wu, Y.-C. Chen, K.-Y. Lee, and S.-S. Shyu, "The ac line current regulation strategy for the grid-connected pv system," *IEEE Transactions on Power Electronics*, vol. 25, no. 1, pp. 209–218, 2009.

[46] Demuth.H.B, Hagan.T.M, and M.H.Beale, *Neural Network Toolbox™ 7 User's Guide*. the MathsWork, September 2010.

[47] H. Demuth and M. Beale, *Neural Network Toolbox For Use with MATLAB*. The MathsWork, october 2004.

[48] C. Touzet, *les reseaux de neurones artificiels, introduction auconnexionnisme*. COURS, EXERCICES ET TRAVAUX PRATIQUES, Jun 2016.

[49] D. Kriesel, *A brief introduction to neural networks*. (ZETA2-EN).

[50] L. P. Jyothy and M. Sindhu, "An artificial neural network based mppt algorithm for solar pv system," in *2018 4th International Conference on Electrical Energy Systems (ICEES)*, pp. 375–380, IEEE, 2018.

[51] V. Skorpil and J. Stastny, "Neural networks and back propagation algorithm," *Electron Bulg Sozopol*, pp. 20–22, 2006.

[52] J. K. M. Jordan and B. Scholkopf, *Pattern Recognition and Machine Learning*. Springer Science+Business Media, pp 241, 2006.

[53] H. M. Malek Benslama, *Compressed Sensing in Li-Fi and Wi-Fi Networks*. ISTE Press - Elsevier, 2017.

[54] M. BOUAZIZ, *Réseaux de neurones récurrents pour la classification de séquences dans des flux audiovisuels parallèles*. PhD thesis, the university of Avignon France, 2017.

[55] M. Gupta, *Soft Computing and Intelligent Systems*. Academic Press, 1999.

[56] V. Devendran, H. Thiagarajan, and A. Wahi, "Novel approach to improve the performance of artificial neural networks," in *2007 International Conference on Signal Processing, Communications and Networking*, pp. 442–445, IEEE, 2007.

[57] Z. Cömert and A. F. Kocamaz, "A study of artificial neural network training algorithms for classification of cardiotocography signals," *J Sci Technol*, vol. 7, no. 2, pp. 93–103, 2017.

[58] N. Pavaday, I. Bhurtah, and K. Soyjaudah, "How to improve performance of neural network in the hardened password mechanism.," *GSTF Journal on Computing*, vol. 1, no. 2, 2011.